FILE NOT INTENDED FOR PRODUCTION

Measuring the elastic modulus of soft culture surfaces and 3D hydrogels using atomic force microscopy

Michael D. A. Norman[1,†], Silvia A. Ferreira[1,a,†], Geraldine M. Jowett[1], Laurent Bozec[2,*], Eileen Gentleman[1,3,*]

[1]Centre for Craniofacial and Regenerative Biology, King's College London, London SE1 9RT, UK

[2]Faculty of Dentistry, University of Toronto, Toronto, ON M5G 1G6, Canada

[3]London Centre for Nanotechnology, London WC1H 0AH, UK

†These authors contributed equally
*To whom correspondence should be addressed:

Eileen Gentleman PhD
Centre for Craniofacial and Regenerative Biology
King's College London
27th Floor, Tower Wing, Guy's Hospital
London SE1 9RT
UK
+44 (0) 20 7188 7388
eileen.gentleman@kcl.ac.uk

OR

Laurent Bozec PhD
Faculty of Dentistry
University of Toronto
124 Edward Street
Toronto, ON M5G 1G6
CANADA
+1 (437) 929-6566
l.bozec@dentistry.utoronto.ca

M.D.A.N.: michael.norman@kcl.ac.uk; **S.A.F.:** s.ferreira@imperial.ac.uk; **G.M.J.:** geraldine.jowett@kcl.ac.uk

[a]Present address: National Heart & Lung Institute, Imperial College London, London SW7 2AZ, UK

KEYWORDS Atomic force microscopy, mechanobiology, substrate stiffness, secreted matrix, Young's modulus, hydrogels, organoids

EDITORIAL SUMMARY This Protocol describes how to use atomic force microscopy to measure elastic modulus of soft 2D surfaces and cell-laden 3D hydrogels. The procedure provides instructions for sample preparation, instrument calibration, data collection and analysis.

TWEET A new Protocol for measuring Young's (elastic) modulus of soft 2D surfaces and cell-laden 3D hydrogels using atomic force microscopy (#AFM #organoid #mechanobiology) @GentlemanLab @L_Bozec.

COVER TEASER Measuring the elastic modulus of 3D hydrogels

ABSTRACT

Growing interest in exploring mechanically mediated biological phenomena has resulted in cell culture substrates and 3D matrices with variable stiffnesses becoming standard tools in biology labs. However, correlating stiffness with biological outcomes and comparing results between research groups is hampered by the variability in methods used to determine Young's (elastic) modulus, *E*, and by the inaccessibility of relevant mechanical engineering protocols to most biology labs. Here, we describe a protocol for measuring *E* of soft 2D surfaces and 3D hydrogels using atomic force microscopy (AFM) force spectroscopy. We provide instructions for preparing hydrogels, with and without encapsulated live cells, and provide a method for mounting samples within the AFM. We also provide details on how to calibrate the instrument, and give step-by-step instructions for collecting force-displacement curves both in manual and automatic modes (stiffness mapping). We then provide details on how to apply either the Hertz or Oliver-Pharr model to calculate *E*, and give additional instructions to aid the user in plotting data distributions and carrying out statistical analyses. We also provide instructions for inferring differential matrix remodelling activity in hydrogels containing encapsulated single cells or organoids. Our protocol is suitable for probing a range of synthetic and naturally derived polymeric hydrogels such as PEG, polyacrylamide, hyaluronic acid, collagen, or Matrigel®. Although sample preparation timings will vary, using this protocol, a user with introductory training to AFM will be able to characterize the mechanical properties of between 2-6 soft surfaces or 3D hydrogels in a single day.

INTRODUCTION

Many cell types mechanically interact with their environment to carry out both normal and pathophysiological behaviours. Cells apply force to their underlying or surrounding matrix, "feel" how much it deforms, transduce this signal, and adapt their response accordingly[1]. Cells' ability to mechanically detect stiffness has been shown to influence numerous behaviours in a myriad of biological contexts, both *in vivo* and *in vitro*. Indeed, cell proliferation, migration, and differentiation[2,3], among other behaviours[4-6], have all been linked to cells' ability to sense the stiffness of their environment. Moreover, the progression and outcomes for some cancers and the pathophysiology of many fibrotic diseases[7] are thought to be at least partially controlled by cells' ability to detect changes in the relative stiffness of their surroundings[8-10].

The word "stiffness" is often used to describe the mechanical properties of cell culture substrates and 3D matrices. However, much confusion arises from its misuse[11]. From a material point of view, stiffness is defined as the resistance of an elastic body to deformation by an applied force. Conversely, the elastic modulus or Young's modulus, denoted as *E*, is a fundamental property of a material that takes its size into account. Therefore, a large block of steel will be stiffer than a thin wire formed from the same material, but their *E* will be identical. In this protocol, we use "stiffness" to refer to general concepts and reserve *E* for specific reference to values of the material property.

Because of this confusion and as different approaches are often applied to determine *E*, definitive values that drive biological processes or promote specific cellular behaviours are uncertain. Moreover, although measurements of *E* need to be performed contextually for each sample, a lack of a homogenized approach has led to reports of widely differing values for what should be identical materials. This is of particular concern, as mechanobiological insights have translational potential for regenerative medicine. Indeed, tissue engineering scaffolds can be designed with mechanical properties to direct seeded or endogenous cells; however, without a consensus on values for *E* that promote particular cellular responses (like differentiation down particular lineages), the precise design criteria needed to translate these findings into therapies is lacking.

Here, we describe a relatively simple method to experimentally measure and calculate the *E* of soft cell culture surfaces and 3D hydrogels applicable for mechanobiological or matrix remodelling studies. Our protocol uses atomic force microscopy (AFM) force spectroscopy, a method whereby a material's surface is indented using a soft cantilever, whose deflection is detected by a laser beam. Since its development, AFM has been successfully used to quantify tissue and substrate mechanics both at the nano and micro scale[31]. As such, AFM is the most widely available system capable of providing highly sensitive mechanical measurements at the scale at which single (or a few) cells "feel" their matrix[31]. We present alternative techniques, discuss the limitations of the technique, and give example materials for which our protocol is appropriate. Finally, we provide a detailed protocol that has been used successfully in the authors' laboratories, which highlights critical steps and pitfalls, and details approaches to interpret expected results.

Development of the protocol

Thompson first reported in 1942 that cells and tissues responded differentially to mechanical cues from their surrounding environment[12], and researchers have known since at least the 1970s that many cell types behaved differently when cultured on soft compared to stiff surfaces[13]. However, it wasn't until the late 1990s when Pelham and Wang[14] created protein-functionalized polyacrylamide (PA) hydrogels, whose *E* could be modulated by changing the concentrations of monomer and cross-linker, that robust experimental approaches capable of systematically studying the response of cells to substrate stiffness were adopted. Using this system, they and others reported that on stiff surfaces cells tend to adopt spread morphologies; develop large, stable focal adhesion plaques; form defined actin stress fibres; and generate large traction forces. In comparison on soft surfaces, cells are often more motile, adopt more round morphologies and fail to assemble either robust actin stress fibres or stable focal adhesion plaques (Fig. 1a and b, for a review, see[15]). Using PA hydrogels, researchers have shown that in identical serum conditions, substrate *E* alone can direct human bone marrow stromal cell (hMSC) differentiation[2]. We have since used the PA system to both demonstrate that hypoxia impacts hMSC response to substrate stiffness during chondrogenic differentiation[16], and to interrogate how physicochemical cues such as stiffness impact T cell activation[17].

More recently, the role of stiffness in directing cell behaviour has been extended to modifiable 3D systems formed from biocompatible hydrogels that allow for cell encapsulation[18,19]. Seminal work by Mooney and colleagues demonstrated that in non-degradable, ionically cross-linked alginate hydrogels, stiffness regulates an hMSC fate switch between adipogenesis and osteogenesis[18]. However, encapsulated cells are not simply passive sensors of matrix cues. They also actively modify their surroundings by secreting and arranging matrix components pericellularly (Fig. 1c)[20]. Indeed, we and others have shown that encapsulated hMSC remodel their pericellular matrix by changing both its composition and stiffness, which drives lineage specification[21,22]. Moreover, we have shown that human induced pluripotent stem cell (hiPSC)-derived intestinal organoids have the capacity to secrete matrix proteins and matrix-cleaving enzymes when encapsulated within PEG hydrogels (Fig. 1d), and that they modify the mechanical properties of their surroundings when stimulated by co-culture with type 1 innate lymphoid cells[23].

This growing interest in mechanobiology has opened the floodgates to new hypotheses, suggesting roles for mechanical cues in the regulation of processes ranging from development[24] to cancer cell biology[8,9]. As a result, it has become standard practice to develop culture platforms with modifiable stiffnesses and correlate biological outcomes with *E*. For example, muscle stem cells are reported to optimally self-renew on surfaces with an *E* of 12 kPa[25]. However, in reality, the methods for measuring and calculating *E* can vary tremendously, making it difficult to compare absolute values across different studies.

The mechanical properties of soft hydrated materials, such as hydrogels and biological tissues, are particularly difficult to determine accurately. For example, reported values of *E* for human

cornea range from <3 kPa to >19 MPa when measured using different methods[26]. Surprisingly, this variability can even extend to the reported *E* of highly defined cell culture substrates[27]. For example, Corning's Sylgard® 184, a formulation of the elastomer polydimethylsiloxane (PDMS) can be functionalized for cell culture, and its *E* can be varied by changing cross-linker concentration[28]. However, reports of *E* for Sylgard® 184 with identical cross-linker concentrations vary depending on the testing method. When tested by nano-indentation, the *E* for a 100:1 formulation has been reported to be 0.1 kPa[29], but when probed by AFM, values range from 41 kPa[3] to 245 kPa[30]. Variations in reported values for *E* can have important implications for biological studies. Indeed, the application of differing methods for determining the *E* of PDMS has resulted in widely different interpretations of the mechanistic basis of cellular mechanotransduction[29,30].

…AFM force spectroscopy is a well-established technique widely used to characterize the mechanical properties of dry, and often hard materials. To develop a protocol for use on soft hydrated materials, changes to standard experimental setups and measurement parameters were required. Performing measurements in liquid are particularly challenging because they require that the sample remains fully hydrated during testing and that the cantilever is stabilized in liquid, which is essential for reducing background noise. Careful sample preparation is also vital to ensure a flat even surface is available to indent. Moreover, when moving from indenting hard substrates to much softer materials, probe shape and indentation parameters need to be carefully adapted.

Overview of the Procedure

The procedure described in this Protocol guides users to perform AFM force spectroscopy measurements to determine the *E* of 2D surfaces and 3D hydrogels, including those containing encapsulated cells or organoids. We start in the 'Experimental design' section by discussing how to choose the correct cantilever and probe, as well as experimental considerations when measuring *E* on hydrogels encapsulating live cells or organoids. We then summarize how to prepare samples in 'Reagent Setup', using 2D PEG surfaces and human intestinal organoids encapsulated within PEG-based hydrogels as exemplar systems. We next cover how to establish an appropriate instrument setup for making measurements. This includes instructions for 'Mounting the cantilever' (Steps 3-7), 'Alignment of laser and photodiode' (Steps 8-11) and 'Mounting a bead on a cantilever' (Steps 12-25). We then provide a detailed strategy to calibrate the cantilever ('Calibration of the Cantilever' (Steps 26-35)). Calibration allows for the conversion of vertical deflection into units of force, which is essential to ensure accurate *E* measurements. Since for hydrogels, *E* should be measured in liquid, we describe how to stabilize the cantilever in liquid, which is essential for re-calibrating the photodiode sensitivity (Steps 36-43). We then explain how to mount 2D and 3D hydrogel samples on the AFM ('Mounting the sample', Steps 44-50), and how to optimize testing parameters to collect force-displacement (*F-D*) curves ('Carrying out *F-D* measurements' Steps 51-68) both in manual and automatic (mapping) modes. We finally highlight how to complete a session (Steps 69-76), and in Steps 77-87, we cover methods for analyzing *F-D* curves to obtain *E*. Finally, we present different ways in which the data can be presented in Steps 88-90.

Comparison with other methods

Methods regularly employed to measure *E* of soft culture surfaces and hydrogels include bulk methods, such as tensile/compressive testing and rheology, and indentation methods. In selecting a method to measure the *E* of materials in the context of cellular mechanosensing or mechanotransduction, it is important to consider the scale at which a single cell "feels" its matrix, and interrogate the material in a similar manner. That is, cells can attach to surfaces or their surrounding matrices and generate tension through their cytoskeleton to mechanically deform their extracellular surroundings. Therefore, understanding the stiffness that a cell "feels" likely requires measurements of the stiffness of a material on a scale similar to the size of a cell.

Bulk methods to determine mechanical properties are either based on compressing or stretching (tensile) a piece of the material (>1 cm). In general, a bulk material is deformed a defined amount and the material's resistance to the deformation (force) is measured. For example, rheological properties are often measured in rotational devices in which a sample is placed between one fixed and one oscillating plate. The angular position is taken as a measure of strain, and the torque, which measures the sample's resistance to deformation, is used to measure storage (G') and loss (G'') moduli, which can be converted to *E*. However, measurements of bulk properties of a material can often vary widely from that captured at a smaller scale[32] Moreover, bulk methods often fail to identify inhomogeneities in the material. For example, we have shown that cells and organoids encapsulated within hydrogels can modify the mechanical properties of their surrounding matrix[21,23], an effect that would not have been captured using bulk mechanical testing methods.

Rheological properties can also be measured using microrheological methods, in which either the Brownian motion of embedded beads is imaged and mechanical properties calculated using the Generalised Stokes-Einstein Relation[33], embedded beads are actively moved within the material[33,34], or solid-to-fluid jamming behaviour is derived from the deformation of oil microdroplets[35]. Other non-contact, imaging-based methods include optical coherence elastography[36], Brillouin microscopy[37], magnetic resonance elastography[38] and ultrasonic shear wave elastography[39]. However, while passive microrheology methods provide micro-level measurements of material properties, they are often limited to extremely soft materials (<~4 Pa)[40]; and active microrheology and imaging-based methods require specialist experimental setups.

The alternative to bulk measurement techniques is to investigate a small area of a material by indenting it with a probe and measuring its resistance to the indentation. Indentation measurements using small probes only measure a small volume of material. Consequently, numerous measurements are required to understand the material's general response and careful attention is required if either the material's surface has different properties than the bulk or if inhomogeneities in *E* are expected[41]. An AFM can be equipped with either nano- or micro-sized tips. Nano-sized tips have the drawback that they may probe either the bending properties of individual polymer molecules or that of their associated water. Micro-sized probes, on the other hand, will probe the mechanical properties of a local network of polymer chains with its

associated water. This scenario can reasonably be assumed to capture the stiffness sensed by a cell probing its surroundings via integrins.

Applications of the method

The protocol we provide can be applied to both 2D and 3D surfaces, ranging from PA hydrogels covalently linked to glass coverslips to functionalized PEG networks crosslinked through Michael-type additions. This extends to other crosslinking strategies and synthetic materials, though caution is warranted on very soft PDMS surfaces (such as Sylgard® 184 with a cross-linker : base ratio of 100:1) because of potential adhesion between the AFM probe and the elastomer surface[32]. Similarly, the protocol is applicable to naturally derived polymeric hydrogels, including those formed from alginate, collagen, fibrin, and Matrigel®. It can also be applied to cultures that have been chemically fixed, however, paraformaldehyde or methanol-based crosslinking may affect the mechanical properties of biological samples, and so resulting measurements should only be interpreted in this context. Our method can also be applied in conjunction with other techniques such as fluorescence microscopy. On AFM systems with epifluorescence capabilities or equipped with confocal lasers, this would allow for correlative measurements of stiffness with localization of fluorescently labelled cells, proteins, particles, or materials[59].

Importantly, we also propose that our method can be used on cell-laden hydrogels. We have successfully applied our protocol to infer pericellular and peri-organoid matrix mechanics in live cultures encapsulated within hydrogels. Here, it should be noted that AFM, in general, is a surface characterization technique. However, on materials like hydrogels, indentations with a spherical probe will result in deformation many microns deep into the hydrogel[60]. Thus, the resulting mechanical response will be that of a combination of the overlying hydrogel, the cells or organoids themselves, and their surrounding matrix[59]. In this way, the technique does not provide a direct measure of the pericellular or peri-organoid *E*. Instead, the complex indentation of cells or organoids embedded within a 3D hydrogel is akin to the Hookean concept of springs in series, which is well known in the field of mechanics. This concept explains that when a mechanical load is applied to springs with spring constants k_1, k_2, ..k_n in series, the mechanical response of the system will be a combination of k_n springs' mechanical properties. Here, k_1 can be thought of as the mechanical properties of the hydrogel and k_2, ..k_n would represent any combination of the stiffnesses of embedded cells, multicellular organoid structures, secreted ECM, and degraded hydrogel (Fig. 2). This model has been experimentally verified using AFM-based force spectroscopy measurements on microglial cells cultured on soft PA substrates (0.05-1 kPa), whereby indentations measured on overlying cells were impacted by deformation of the underlying substrate, which impacted calculations of *E*[60].

The springs in series concept cannot determine the absolute values for *E* of the underlying organoids/cells/matrix from AFM measurements alone. More sophisticated measurements and analyses combining AFM force spectroscopy with confocal microscopy, finite element simulations and analytical modelling do allow direct measures of cell and pericellular matrix stiffness to be extracted from such data[59]. Nevertheless, our technique does enable valuable comparisons of specific experimental conditions. For example, our protocol allows for net

differences in mechanical properties induced by increased matrix deposition or enzyme-mediated hydrogel degradation to be detected[23]. However, caution is urged in interpreting data collected on such complex biological systems, as many factors will influence the measurements. For example, inferring pericellular mechanics around encapsulated organoids and spheroids is likely to be strongly influenced by the cellular structures themselves. For instance, gut or lung organoids often form an epithelial monolayer surrounding a liquid-filled pseudolumen structure, while neural spheroids or embryoid bodies are comprised of dense cellular aggregates. Thus, we advise against comparing the behaviour of different cell types, even if they all form 3D aggregates. One strategy to mitigate this would be to conduct AFM measurements directly on cryosections[61]. However, the user would need to balance the benefit of direct measurements of pericellular/peri-organoid stiffness against the drawbacks of devitalized cultures that have undergone processing and sectioning.

Limitations

Although our protocol is applicable to commonly used modifiable cell culture substrates and many hydrogels used for cell encapsulation, there are some cases when it should not be applied. For a material or surface to be accurately probed, it must be sufficiently thick that the stiffness of the underlying support does not impact measurements[62,63]. As a general rule, the effect of the underlying hard substrate is negligible if the indenter penetration is less than 10% of the material's thickness[64,65]. Not only is consideration of gel thickness important for determining hydrogel mechanical properties, but also for drawing conclusions regarding cell behaviour. This is because cells cultured on soft, thin hydrogels, such as those formed from PA (whose basal side is often covalently linked to a glass coverslip for ease of handling), will behave similarly to cells on stiffer hydrogels. Indeed, cells on very thin soft gels will "feel"[66,67] the underlying hard glass substrate just as in the fairy tale *The Princess and the Pea*, in which the princess feels a hard pea under a large stack of mattresses[1]. In general, most single cells (as opposed to colonies, which can exert more traction[67]) will "feel" the underlying glass substrate if the thickness of the PA hydrogel is less than ~15 to 40 μm

The testing method and theoretical model we present here are optimized for hydrogels that meet the assumptions of the Hertz/Oliver-Pharr models. That is, materials that behave linearly elastically and are isotropic. PA and PEG hydrogels, for example, behave as linearly elastic (or poroelastic) materials at small strains. Materials that are viscoelastic do not obey these assumptions, and so applying these analytical constructions are not appropriate[68]. This protocol should not be applied to measure the mechanical properties of live mammalian cells cultured on 2D surfaces. Mammalian cells can display viscoelastic behaviour and so applying the linear elastic contact models we describe here are not appropriate. The reader is instead referred to[58,69,70], which describe methods for making such measurements. Moreover, this protocol does not include instructions to simultaneously combine imaging and force spectroscopy measurements, such as Quantitative Imaging or Quantitative Nanoscale Mechanical Characterization. Such methods are not suitable when using a colloidal probe.

Expertise needed to implement the protocol

As with any microscopy technique, AFM requires a moderate level of expertise to perform accurate measurements. It can be challenging for new users to work with hydrogels in a liquid environment. However, since AFM is only used to perform *F-D* measurements in this protocol, training in imaging modes is not necessary. Any user should be able to follow the steps of this protocol and obtain high-quality *F-D* curves. AFM instruments vary and so training in operating any individual AFM will need to be provided by a skilled user.

Extracting *E* from data can either be done in proprietary software that runs on AFM instruments or will require Matlab and basic skills with the software package to execute our user-friendly code (https://github.com/eileengentleman/AFM-code). Many universities run short courses in Matlab that would be sufficient to allow an inexperienced user to execute the code. Alternatively, web-based courses/instruction videos (Ledeczi, A. & Fitzpatricl, M., Introduction to programming with MATLAB, Available at https://www.coursera.org/learn/matlab, (2020)) should allow anyone to gain enough skills in Matlab to analyze AFM-generated *F-D* curves and calculate *E* (JPKInstruments, Determining the elastic modulus of biological samples using atomic force microscopy, Available at https://www.jpk.com/app-technotes-img/AFM/pdf/jpk-app-elastic-modulus.14-1.pdf, (2020)).

Experimental design

Choosing the AFM equipment

In-liquid AFM-based measurements are ideal for studying the mechanical properties of soft, hydrated materials. AFM stages can be mounted on inverted or upright microscopes, or inverted confocal microscopes to provide complementary information from the sample, including spatial information and biological readouts using standard fluorescence techniques. Conducting measurements using a closed feedback loop also ensures precise positioning in the X, Y and Z dimensions to correlate *E* with images. For measurements over large areas (>100 µm x 100 µm), AFM heads can also be mounted onto motorized stages, to allow stiffness maps to be collected. For particularly uneven or adhesive samples, AFM heads with a long Z-length (*e.g.,* 100 µm) can make measurements easier by ensuring that the tip fully disengages from the sample following indentation. For the development of this protocol, we used either a JPK (now Bruker) Nanowizard 1, a JPK Nanowizard 4 or a JPK Nanowizard CellHesion; however, the basic steps are largely applicable to other AFM systems operating on an inverted microscope, such as Flex-Bio AFM (Nanosurf), MFP-3D-Bio™ AFM (Asylum Research, Oxford Instrument), 7500 ILM AFM (Keysight Technologies), Park NX-Bio AFM (Park Systems), BioScope Resolve™ AFM (Bruker), and NTEGRA Life (NT-MDT Spectrum Instruments). AFM setups should be mounted on an anti-vibration table/unit, and if possible, in an acoustic chamber to minimize noise.

Choosing an appropriate tip

When probing hydrated hydrogels, the choice of probe will impact the nature of the measurement, and thus must be accounted for when choosing the theoretical model to calculate *E*. Conical or pyramidal pointed tips, whose contact area can be similar in size to the theoretical mesh size of a hydrogel[42,43] are likely to penetrate[44] rather than indent. Colloidal probes (*i.e.*,

tipless cantilevers functionalized with a glass or polystyrene sphere), on the other hand, contact the material over a larger area, making it possible to probe the stiffness of hydrogel networks, but with the drawback that spatial resolution is compromised. Resolution is defined by the contact area between the probe and the sample, and so using a colloidal probe necessitates a compromise between bead diameter, contact area, hydrogel mesh size and spatial resolution. Probes can be purchased with the bead pre-mounted or manufactured at low-cost by the user. The diameter of the sphere will determine the contact area between the probe and sample. Very soft materials (~1 kPa or softer) require larger beads to avoid penetrating the material rather than indenting it. When inferring pericellular or peri-organoid stiffness, larger beads are also advised, as they allow for a deeper indentation and thus measurements of mechanics on a larger scale. For stiffer materials, smaller spheres will allow more precise measurements of local stiffness values. We have applied our protocol with beads ranging from 10-75 μm in diameter; however, care must be taken when attaching large beads to soft cantilevers as their weight can impact cantilever calibration and deflection measurements. In addition to size, it is also important to consider the bead's material composition; while glass beads may adhere less to some samples compared to polystyrene, they can be heavier, similarly limiting the size of the bead that can be placed on a soft cantilever.

Selecting and calibrating a suitable cantilever

AFM cantilevers with pre-calibrated spring constants can be purchased from various suppliers. The cantilever's spring constant should be selected such that it closely matches the expected stiffness range for the material being probed. If the spring constant of the cantilever is too low (or "soft"), the cantilever will bend easily without indenting the material. However, if the spring constant of the cantilever is too high (or "stiff"), the cantilever will indent the material without deflecting. If the sample's approximate elasticity is unestablished, it is advisable to begin with low-spring constant cantilevers and gradually increase the value of the spring constant until a suitable indentation is obtained. Biologically derived hydrogels (Matrigel®, collagen gels, *etc.*) have stiffnesses in the range of <1 kPa, so 0.01-0.06 N/m cantilevers are often appropriate. For many synthetic hydrogels, which can be made stiffer (*i.e.* 1-10 kPa and higher), spring constants of 0.1-0.3 N/m should provide sensitive readings.

Once a cantilever has been chosen, calibration is critical for obtaining accurate measurements of *E*. In particular, two key parameters need to be calculated: the *deflection sensitivity* and cantilever's *spring constant*. The deflection sensitivity is unique to each AFM system and needs to be measured before each experiment. The deflection sensitivity (nm/V) is the constant ratio between cantilever deflection (in nm) and its resulting voltage generated by the 4-quadrant photodiode. The deflection sensitivity is the largest source of variability when calibrating cantilevers[45]. Therefore, special care must be taken when measuring it. In particular, clean sample surfaces and cantilever tips are essential. After measuring deflection sensitivity, there are several strategies to calculate the cantilever's spring constant, which include using the cantilever's geometry[46]; applying the added mass method[47]; and relying on a reference cantilever[48-50]. However, the thermal noise method[51] is most commonly applied as it is convenient, requiring no additional equipment, and does not risk damaging the cantilever. It is

also highly suitable for cantilevers with spring constants of <1 N/m[52], and only requires the user to additionally input temperature and cantilever tilt to correctly calculate the spring constant.

Overall, ensuring calibration is carried out carefully and consistently will reduce variability. As an alternative to the cantilever calibration procedure described in Steps 26-35 of this protocol, users might also consider newer methods, such as the Standardized Nanomechanical Atomic Force Microscopy Procedure (SNAP)[45], which calculates the cantilever's spring constant and sensitivity using an external instrument (*e.g*, a vibrometer), which may reduce variability associated with measurements of the cantilever's deflection sensitivity via the standard indentation method. The user may also wish to confirm correct calibration using commercially available reference samples of a known *E* (*e.g.* Petrisoft 35, cat. no. PS35-EC-0.2 PK)).

Preparing a loading regime

Determining *E* from *F-D* curves collected by AFM requires the indentation of the cantilever into the sample to a depth of no more than 10% of the sample thickness. As a rule, parameters should be adjusted so that on thin samples, the underlying substrate does not influence stiffness measurements, but the indentation depth is still sufficient to observe a response from the network. For many mechanical models, the indentation depth in relation to probe radius is assumed to be small, thus indentation depth should not comprise more than 1/3 of the bead radius. This means that for a 10 μm-diameter bead, indentations deeper than 1.6 μm should be avoided. In our experience, an indentation depth between 100-1500 nm on samples that are at least 25 μm thick provides good measurements of *E*. We advise against applying this protocol to samples thinner than ~25 μm.

Although many synthetic materials are theoretically homogenous, inhomogeneities may still exist, and environmental interference as well as other factors may influence individual measurements. For this reason, to obtain an accurate measure of *E*, the material should be probed numerous times at random locations (we suggest 10 x 10 grids in 100 μm x 100 μm maps in 6 locations across the surface, 600 *F-D* curves). This will ensure measurements of the distribution of *E* across the sample.

Choosing an appropriate model

Calculating *E* from *F-D* curves requires fitting the experimental data with a theoretical model. Models rely on assumptions about the material and how both it and the probe will interact during the indentation cycle. Whilst beyond the scope of this protocol, the wide variety of mechanics models that can be applied are discussed in depth in reviews such as [53] and [54].

One of the most common models to calculate *E* is the Hertz model, which describes the indentation of an elastic half-space. Important assumptions within this model are that the indentation is frictionless, strains are small (*e.g.,* contact area [A_c] remains much smaller than the probe radius [A_c<<R]), and that the deformation is linearly elastic. Whilst these assumptions hold for many hydrogels when probed using appropriate testing parameters, this model can begin to break down for soft materials with large deformations[53]. Moreover, for some measurements, the probes' radius can also limit indentation depths whilst still meeting the

requirement for a low A_c/R ratio. One way this can be partly circumvented is through application of the Oliver-Pharr model.

The Oliver-Pharr model, developed using Sneddon's analytical approach for a punch indenter[55], assumes an elastic-plastic indentation with elastic relaxation occurring in the initial part of the unloading curve. Importantly, the projected indenter contact area is calculated from the indentation depth (Supplementary Note 1). This correction potentially makes the Oliver-Pharr model more suitable for deformations at large indentation depths (*i.e.,* larger A_c/R ratios). Within most AFM software, there is already the capability to calculate *E* using the Hertz model. However, modelling *F-D* curves with Oliver-Pharr requires an external script, and so herein we include a Matlab script to calculate *E* using this model. However, care must also be taken when applying the Oliver-Pharr model. As it is fitted to the unloading curve, tip-sample interactions can influence the initial portion of the unloading curve and thus can impact results.

For materials in which there is adhesion between the probe and the sample, other models such as Derjaguin-Muller-Toporov (DMT) and Johnson-Kendall-Roberts (JKR) should be considered[56]. The JKR model accounts for adhesion forces within the contact area whereas the DMT model takes into account adhesive forces away from the contact area[57]. Therefore, the JKR model may be more appropriate when relatively large indentors are used to probe samples that display strong adhesive properties. The DMT model, on the other hand, is valid for stiffer materials, smaller probes and materials with weaker adhesive properties.

Some hydrogels and cell culture surfaces, particularly those formed from biological polymers, may exhibit viscoelastic behaviours. Often the impact of viscoelasticity can be negligible for small fast indentations; however, alternative models can also be applied to take these time-dependent behaviours into consideration. For example, poroelastic models[44] can account for fluid movement through the hydrogel during indentation; however, they often require additional physical characterization (*e.g.*, hydrogel permeability, k) which can be experimentally and/or theoretically challenging to determine.

Considerations for live samples

3D materials containing live encapsulated cells or organoids present additional challenges[58], and factors such as the composition of the medium and temperature become important additional considerations. Many cultures are grown in medium containing serum whose proteins can adsorb to the tip of the cantilever, potentially impacting measurements. Therefore, for measurements on live cultures, it is advisable to replace serum-containing medium with serum-free physiological buffer prior to measurements. Although AFM systems can be placed in environmental chambers and measurements conducted under sterile conditions, such setups are not common. We have instead optimized this protocol for AFM systems in open labs and thus most will be end-point only. In such open environments, CO_2-independent medium can also be used to help regulate pH under atmospheric conditions. Similarly, plate heaters can be included on AFM setups to maintain physiological temperatures. When using AFM to infer pericellular or peri-organoid matrix remodelling, it is also important to create thin samples (*i.e.* hydrogel thickness no more than 2-3X the diameter of largest organoid). This minimizes the distance between the hydrogel surface and encapsulated cells or organoids to maximize the

ability of the technique to detect their contribution to *E*. In general, and especially when not using CO_2 or temperature control it is advisable to carry out AFM measurements in under 1-2 h to minimize the impact of environmental conditions on cellular responses, though sensitivity to CO_2 and temperature will vary depending on cell type.

MATERIALS

Biological Materials

- Organoids can be derived from many primary proliferative tissues or from hiPSC using well-established protocols[78], and should be cultured in appropriate media. Here, we discuss how to encapsulate hiPSC-derived intestinal organoids matured in Matrigel prior to hydrogel encapsulation[23].

  ! CAUTION Informed consent must be obtained for experiments involving human tissues and cells. Experiments must conform to all relevant institutional and governmental regulation.

  ! CAUTION The cell lines used in your research should be regularly checked to ensure they are authentic and are not infected with mycoplasma.

Reagents

! CAUTION When handling the chemicals used in this protocol, always wear suitable personal protective equipment. For any chemical listed in this protocol, appropriate institutional and governmental safety guidelines must be followed. Please refer to the appropriate materials safety data sheets.

! CRITICAL This protocol can be used to perform AFM measurements on a variety of 2D soft surfaces and 3D hydrogels formed using different materials (*e.g.*, PA[16,17,73], S-HA-PEGDA[21,74,75]), either as acellular materials or containing encapsulated cells. In addition to the setup described below, we have successfully used this protocol on both acellular PA hydrogels and S-HA-PEGDA hydrogels containing encapsulated hMSC; however, the protocol can also be applied to other hydrogel materials with or without encapsulated primary mammalian cells, cell lines or organoids. Here, we detail the reagent setup to perform AFM measurements on 4-arm PEG hydrogels crosslinked with custom-designed peptides, similar to those described by others[76,77], and as described by Jowett *et al*[23]. We describe the reagents and setup both to form these hydrogels as 2D surfaces, and to use them to encapsulate human intestinal organoids.

PEG hydrogel formation

- Sigmacote (Sigma, cat. no. SL2)
- Hydrogel precursor components (*e.g.,* 4-arm PEG-vinyl sulfone (JenKem, cat. no. 4ARM-VS) and PEG-peptide conjugates) as described previously[23]
- HEPES buffer powder (*e.g.,* Sigma, cat. no. H4034)
- Hank's Balanced Salt Solution (HBSS), 10× (*e.g.* ThermoFisher, cat. no. 14065056)

- Phosphate buffer saline (PBS, pH 7.4, no calcium, no magnesium, Gibco, cat. no. 20012068)
- Sodium hydroxide solution (NaOH)

Human intestinal organoid (HIO) culture

- Matrigel (BD Biosciences, cat. no. 354234)
- Advanced DMEM/F12 (Invitrogen, cat. no. 12634-010)
- B27 (50×) supplement (Invitrogen, 17504044)
- L-glutamine (100×) (Invitrogen, cat. no. 25030-081)
- Pen/Strep (100×) (Invitrogen, cat. no. 15140-122)
- Hank's Balanced Salt Solution, pH 8 (HBSS, *e.g.,* Gibco, cat. no. 14025092)
- HEPES Buffer, pH 8 (Invitrogen, cat. no. 15630080)
- Epidermal Growth Factor (R&D Systems, cat. no. 236-EG)
- R-spondin-1 (R&D Systems, cat. no. 4645-RS)
- Noggin (R&D Systems, cat. no. 6057-NG)
- Cell recovery solution (Corning, cat. no. 354253)
- Phosphate buffer saline (PBS, pH 7.4, no calcium, no magnesium, Gibco, cat. no. 20012068)
- HIO formed from Kute-4 human induced pluripotent stem cells[78] (ECACC, cat. no. 77650426, RRID:CVCL_EF20)

AFM measurements

- CO_2-independent serum-free media (Thermofisher, cat. no. 18045054)
- Phosphate buffer saline (PBS, pH 7.4, no calcium, no magnesium, Gibco, cat. no. 20012068)
- Ethanol, absolute (Merck, cat. no. 1070172511). **! CAUTION** Ethanol is flammable and can cause moderate eye and skin irritation. Always handle whilst wearing personal protective equipment and keep away from open flames and hot surfaces.

EQUIPMENT

Hydrogel formation and HIO encapsulation

- Low-rim 35 mm tissue culture treated dishes (glass-bottom or plastic, *e.g.,* TPP, cat. no. 93060). **Δ CRITICAL**: The height of standard tissue culture plates or wells smaller than 35 mm will exceed the range and width accessible by the AFM probe.
- Round plastic coverslips, 13 mm diameter, sterile, pyrogen-free (Starlab, cat. no. 83.1840.002)
- Standard equipment for mammalian cell culture
- Sterile moulds (*e.g.,* autoclaved 6 mm borosilicate glass cylinder moulds, Bellco, cat. no. 2090-00608)
- Vortexer
- Forceps

- 22 mm glass coverslips (*e.g.,* VWR, cat. no. 631 - 1089)
- Protein low-binding eppendorf tubes (*e.g.,* Eppendorf, cat. no. 0030108116)
- Protein low-binding pipette tips (*e.g.,* Corning DeckWorks, cat. no. CLS4151)

Cantilever preparation

- Tipless triangular silicon nitride cantilevers (Bruker AXS SAS, K » 0.06-0.35 N/m, cat. no. NP-O10, or Bruker AXS SAS, K » 0.01-0.6 N/m, cat. no. MLCT-O10, see 'Selecting a suitable cantilever')
- Microbeads, spherical glass microbeads (Cospheric, cat. no. S-SLGMS, 50-53 µm (diameter), or Whitehouse Scientific, cat. no. MSS010 10 µm silica microspheres, or 37.28 µm Polystyrene microspheres (Microparticles GmbH, cat. no. PS-R-37.0))
- Uncoated glass microscopy slides (Sigma, cat. no. CLS294775X50)
- Precision wipes (Kimwipes, Kimberly-Clark)
- Lens tissues (Watman, cat. no. 105)
- UV curable glue (Loctite, cat. no. AA350)
- Glass block cantilever holder (JPK Instruments AG, cat. no. JPK SP-90-05).
- Immunohistochemistry hydrophobic barrier PAP pen (Vector labs, cat. no. ImmEdge H-4000)
- Forceps with plastic tips (Cole-Parmer, cat. no. 00CF.SA.1)
- Spatula (Fisher Scientific, cat. no. S50788A)

AFM setup

CRITICAL: We have developed our protocol with the following three AFM setups. Alternative setups that should be compatible with our protocol are described in Experimental Design - Choosing the equipment.

- JPK (now Bruker) NanoWizard® 1 AFM combined with a wide-field inverted Olympus IX71 inverted microscope placed on an active anti-vibration table and controlled with JPK Scanning Probe Microscopy (SPM) software 5.0 (JPK Instruments AG). Hamamatsu ORCA ER combined with Micro-Manager software allows optical image acquisition.
- JPK NanoWizard® 4 AFM combined with a wide-field inverted Olympus IX71 inverted microscope placed on an active anti-vibration table and controlled with JPK Scanning Probe Microscopy (SPM) software 6.1 (JPK Instruments AG).
- JPK CellHesion 200 AFM with an inverted Olympus IX73, equipped with a motorised precision stage, placed on a TMC active anti-vibration table, and controlled with JPK Scanning Probe Microscopy (SPM) software 5.0 (JPK Instruments AG)

Additional equipment for AFM measurements

- Plasticine (Bostik)
- Binocular stereomicroscope with 20x magnification (Leica, cat. no. 10447198)
- Vibration isolation platform such as an air table (TMC Active Antivibration Table) or benchtop isolation unit (Accurion i4 series Active Vibration Isolation unit)
- Acoustic hood (JPK Acoustic Enclosure), optional

- UV mercury vapour lamp, intensity 20 mW/cm^2, output wavelength 365 nm. **! CAUTION** UV lamps are a source of UV radiation that can damage unprotected eyes and skin. Always wear protective glasses, a lab coat and gloves when working with UV light.

Software

- Micro-Manager software (https://micro-manager.org/)
- AFM software (specific to the experimental setup, *e.g.,* SPM 6.0 JPK BioAFM, Bruker, https://www.jpk.com)
- MATLAB R2019a or higher (Mathworks, https://www.mathworks.com)
- MATLAB-based analysis code (https://github.com/eileengentleman/AFM-code and Supplementary Note 1)
- OriginPro 8 SR0 software (OriginLab Corporation, https://www.originlab.com)
- GraphPad Prism version 8 or higher (GraphPad Software https://www.graphpad.com/scientific-software/prism/)
- IBM® SPSS® statistics version V23 (IBM, https://www.ibm.com)

REAGENTS SETUP

CRITICAL The Reagents Setup details the dissociation of 1 well of Matrigel-embedded HIO (from a 24-well plate) for encapsulation within 2 x 30 µL PEG-based hydrogels.

HBSS/HEPES buffer (pH 8)

Using HEPES powder and 10× HBSS, prepare a 1× HBSS (30 mM HEPES) solution. Correct the pH to 8 using NaOH solution before achieving the final volume. This buffer can be stored at 4 °C for up to 6 months. **Δ Critical** Most cells tolerate non-physiological pH for a short period of time, however, for cell types that are particularly sensitive to pH, the pH of the HBSS/HEPES buffer can be adjusted to 7.85-8.2 to balance speed of hydrogel gelation with cell viability.

Preparation of acellular 2D hydrogel surfaces

1. **Immerse** 22 mm glass coverslips in Sigmacote for 1-2 minutes, remove and allow to air dry, then rinse thoroughly with water to remove any leftover byproducts (explained also in the manufacturer's instructions).
   Δ Critical Step Sigmacote produces an acidic byproduct. It is crucial that coverslips are prepared according to manufacturer's instructions and thoroughly rinsed to ensure that the pH of base-catalyzed hydrogel gelation is not altered.
2. Dissolve appropriate weights of pre-prepared PEG-peptide conjugates and 4-arm PEG-vinyl sulfone in HBSS/HEPES buffer in separate 1.5 mL protein low binding tubes and vortex briefly, as previously described. For example, to create a 2.5% w/v 30µl hydrogel, the total solid mass would be 0.75mg with 50% consisting of the PEG-Peptide conjugate, and 50% the PEG-vinyl sulfone in a 1:1 molar ratio)
3. Using protein-low binding pipette tips, combine 15µl of each solution (for 30µl hydrogel example) in a 1.5 mL protein-low binding tube to achieve equal molar masses of PEG-peptide conjugates and 4-arm PEG-vinyl sulfone and vortex for 5-10 s.

4. Rapidly pipette the solution into the centre of a 6-well tissue-culture treated plate using protein-low binding pipette tips.
5. Gently place the Sigmacote-treated glass coverslip (from Step 1) onto the surface of the hydrogel using forceps.
6. Incubate at 37 ^{o}C for 45-90 min to allow the hydrogel to cross-link.
7. Carefully remove the glass coverslip using forceps. Add sufficient PBS to cover the hydrogel and maintain in PBS until ready to begin AFM measurements.
   PAUSE POINT Acellular hydrogels can be formed in advance and stored immersed in PBS at 4 °C for at least 4 weeks prior to testing.

Culture medium

Prepare complete culture medium by supplementing Advanced DMEM:F12 medium with B27 supplement (1×), L-glutamine (final concentration 2 mM), Pen/Strep (final concentrations: Pen, 100 Units/mL; Strep, 100 µg/mL), HEPES buffer (final concentration 15 mM), Rspondin1 (final concentration 500 ng/mL), Noggin (final concentration 100 ng/mL), EGF (final concentration 100 ng/mL). This medium should be kept sterile and can be stored at 4 °C for 4–6 weeks.

Dissociation of HIO from Matrigel

1. Remove and discard the culture medium around Matrigel-embedded HIO (prepared as described in ref).
2. Rinse the well with 1 mL PBS, and incubate the Matrigel-embedded HIO for 5-10 min in pre-warmed Cell Recovery solution.
   Δ Critical Step While other dissociation methods can be used, these may impact both HIO structure and the integrity of the surrounding extracellular matrix. For example, trypsin/EDTA will dissociate HIO to single cells. Although this may be desirable for certain experiments, in this protocol we seed intact HIO.
3. Collect and quench floating, intact HIO structures in 1 mL ice-cold unsupplemented Advanced DMEM/F12 medium in a 15 mL conical tube.
4. Rinse the well with an additional 1 mL unsupplemented Advanced DMEM/F12 medium and add to the conical tube to ensure full recovery of HIO.
   Δ Critical Step Rinse steps are essential as serum proteins and growth factors can impact hydrogel gelation.
5. Centrifuge the conical tube at 200 g for 5 min at 4 °C. Aspirate supernatant and resuspend pellet in 5 mL PBS.
6. Centrifuge for an additional 5 min at 200 g at 4 °C and rinse with 5 mL ice-cold HBSS.
7. Centrifuge again for 5 min at 200 g at 4 °C and resuspend HIO in the desired volume of ice-cold HBSS in a protein low-binding eppendorf tube.

Preparation of hydrogels

1. **Immerse** 6 mm borosilicate glass cylinder moulds in Sigmacote for 1-2 minutes, remove and allow to air dry, then rinse thoroughly with water to remove byproducts (explained also in the manufacturer's instructions) and autoclave.
   Δ Critical Step Broken, chipped, or incorrectly Sigmacote-treated glass moulds can stick to the hydrogel, damaging it upon removal, which may impact the hydrogel structure and thus AFM measurements.
2. Dissolve appropriate weights of pre-prepared PEG-peptide conjugates and 4-arm PEG-vinyl sulfone in HBSS/HEPES buffer in separate 1.5 mL protein low binding tubes and vortex briefly, as previously described. For example, to create a 5% w/v 30µl hydrogel, the total solid mass would be 1.5mg with 50% consisting of the PEG-Peptide conjugate, and 50% the PEG-vinyl sulfone in a 1:1 molar ratio.
3. Using protein-low binding pipette tips, combine 15µl of each solution (for 30µl hydrogel example) in a 1.5 mL protein low binding tube to achieve equal molar masses of PEG-peptide conjugates and 4-arm PEG-vinyl sulfone and vortex for 5-10 s. The volume and concentration of HIO, 4-arm PEG-vinyl sulfone and PEG-peptide conjugates will vary based on the desired properties of the hydrogel, as well as the desired HIO density.
   ⊗ **Critical Step** Choice of hydrogel volume must allow for a flat surface to be formed. An insufficient hydrogel volume in a large diameter mould can cause the surface to be concave, which can impact AFM measurements.
4. (Optional) Quickly add the organoids (see '**Dissociation of HIO from Matrigel**' above) to the PEG-Peptide conjugate/PEG-VS mix, pipette the solution into a pre-warmed glass mould, and incubate at 37 ^{o}C for 35-45 min to allow the hydrogel to cross-link.
5. Carefully remove the glass mould using sterile forceps, add complete cell culture medium, and culture under standard conditions until ready to perform AFM measurements.

PAUSE POINT Most synthetic, acellular hydrogels can be formed in advance and stored immersed in PBS at 4 °C for at least 4 weeks prior to testing. Many hydrogels swell when placed in aqueous solutions after gelation. It's often advisable to wait until they are fully swollen to make measurements (often 24-48 h). For protein-based hydrogels, long-term stability will depend on protein stability. The stability of cell-laden hydrogels will additionally depend on the growth of the cells and the susceptibility of the hydrogel to degradation.

PROCEDURE

Switch on the microscope ●TIMING ~ 5 min

1| Switch on the main power of the *SPM Control Station* with signal access module, computer and screens, camera, fluorescence box (if necessary), and microscope light for bright field imaging. For most brightfield microscope cameras, these can be operated within the JPK CCD-camera (JUnicam) window; however, for cameras that are unsupported or if more advanced imaging features are required (*e.g.,* fluorescence imaging), these can be opened in a secondary imaging software program such as Micro-Manager.

2| Open the JPK SPM software to control the JPK Nanowizard® AFM. This software has a

Menu bar (where *Stepper Motors* and *Approach Parameters* can be accessed), a *Tool bar* (where *Save, Approach, Retract, Run, Z-Stepper Motor, Laser On/Off, Laser Alignment* and *Measurement Mode* can be accessed), a *Feedback Control* menu (to define *IGain*, *PGain* and *Setpoint*), a *Scan Control* menu (for imaging) or *Spectroscopy Control* menu (for force spectroscopy), a *Z-piezo range display,* and a *System Status Display*. The *Data Viewer* window displays data. Force curves can be viewed in the *Force Spectroscopy Oscilloscope* window.

Mounting the cantilever ●TIMING ~ 15 min

3| While wearing gloves, clean the glass block cantilever holder with absolute ethanol and dry with lens tissue, leaving it free from debris. Check that the prism is clean and has no cracks.

Δ CRITICAL STEP Dust/contamination can impact data quality.

4| Place the manufacture's box containing the cantilever under the stereomicroscope to confirm that the cantilever is intact and clean.

5| Using forceps with plastic tips, grasp a tipless cantilever by the large silicon piece (the chip) to remove it from the manufacturer's box and place it on to the glass block cantilever holder, and secure it in place with the metal clamp using a screwdriver. For some types of cantilever holders, the tip is alternatively held in place with a cantilever spring which is put into place using forceps. For cantilever holders with cylindrical sides, the cantilever should be in the middle of the two grooves, close to the inclined prism edge. For cantilever holders with angled sides, the cantilever should be placed in the centre (Fig. 3a). In every case, the cantilever tip should be positioned over the polished glass end.

Δ CRITICAL STEP Forceps with plastic tips are ideal to avoid scratching the prism. Do not touch the optical surfaces with forceps. Always use gloves and keep the manufacturer's box holding the cantilevers closed to avoid damaging or contaminating the cantilevers.

Δ CRITICAL STEP When using the JPK dish heater, it is essential to use the extended JPK glass block cantilever holder (*e.g.,* JPK SP-90-05).

6| Adjust the glass block cantilever holder to the *AFM Head*. The cantilever holder must be placed into the *AFM Head* so that the cantilever tip is pointing upwards. Turn the glass block by 90 degrees clockwise, orienting the cantilever spring to the left and the cantilever to the right. Lock the glass block in place by moving the two finger grips on the rim of the steel disk.

Δ CRITICAL STEP Handle probes gently and only use moderate force to lock the glass block in place. Avoid handling the glass block as it can break or chip if dropped.

7| Place a clean glass slide in the *Sample Holder.* Ensure that the *AFM Head* is at its maximum *Z-position height* using the *Z-Stepper Motor* and mount the *AFM Head* into its 3-leg position. Ensure that the AFM is in force-spectroscopy mode.

Alignment of the laser and photodiode ●TIMING ~ 5 min

8| Switch on the laser.

9| Using the optical microscope image from the JPK CCD-camera (JUnicam) window, align the laser onto the cantilever using the *Laser adjustment screws* until the beam is directed on the tip of the cantilever.

Δ CRITICAL STEP Depending on the working distance of the microscope, it may be necessary to use the *Z-Stepper Motors* to bring the cantilever into focus.

10| Open the *Laser Alignment* window. This window gives a graphical representation of the detector signal to guide the user to correctly align the laser in the four-quadrant photodiode.
11| Adjust the laser position to the centre of the four-quadrant window, which corresponds to the centre of the *Detector* using the *Detector adjustment screws*. Once centred, gently turn the *Mirror adjustment screw* to optimize the angle of the *Mirror* so that the *Sum signal* is maximized. The *Sum* value is the total signal from all four quadrants of the detector.
Δ CRITICAL STEP The reflected laser must be in the centre of the detector to achieve maximum sensitivity. If the sum signal is low after aligning the laser, the mirror may need to be adjusted first before then adjusting the detector.
! CAUTION Looking into the eyepiece of the inverted microscope during laser alignment can cause eye damage. Only use the optical image from the JPK CCD-camera to align the laser.
? TROUBLESHOOTING

Mounting a bead on a cantilever ●TIMING ~ 40 min
12| On the right side of a glass slide, place a small (~10 µL) drop of UV-curable glue, and then spread it in a thin line using a pipette tip (perpendicular to the long side of the slide) (Fig. 3b).
13| On the left side of the slide, place a tiny number of beads using either a spatula or pipette tip, spreading them to prevent large clumps (for beads in solution ~2-5 µL is sufficient, but this must be allowed to dry before proceeding).
14| Ensure that the *AFM Head* is at its maximum *Z-position height* using the *Z-Stepper Motor.* Switch off the laser. Remove the *AFM Head* and place the glass slide on the *Sample Holder*.
! CAUTION Removing the *AFM Head* before switching off the laser can cause the laser beam to scatter off the instrument, which can cause eye damage. Always switch off the laser using the JPK SPM software before removing the *AFM Head.*
15| Place the *AFM Head* into its 3-leg position and adjust either the *Sample Holder* or *AFM Head* position so that it is above the slide.
16| Using the optical image provided by the camera, position the end of the cantilever tip over the glue by moving the *Sample Holder*. This step is best accomplished using a 10X objective.
17| Switch on the laser and align the laser and photodiode as described in Steps 8-11.
18| Make sure the glue is in focus. Using the *Z-Stepper Motor,* move the tip of the cantilever down until it is close to the glue, but not touching. Then use 5-10 µm steps to lower the tip of the cantilever so that it comes into focus and makes contact with the small drop of glue, confirmation of which will be evident by jump in the vertical deflection of the laser spot in the *Laser Alignment* window.
Δ CRITICAL STEP When using the *Macrometric Focus* to move objectives, always use small movements to prevent the objective from colliding with the sample or cantilever. Long working distance objectives are advised. Equally, avoid using large steps with the *Z-Stepper Motors* (>200 µm) to avoid the cantilever crashing into the slide. Only remove the *AFM Head* or rotate the revolving nosepiece containing the objectives to change the objective if the cantilever is at maximum *Z-position height* and then move the cantilever down carefully, adjusting the focus.
19| Retract immediately to remove the tip from the glue.
Δ CRITICAL STEP Use as little glue as possible. Ensure that only the very end of the cantilever tip is dipped in the glue. Excess glue can be removed by slowly approaching a clean area of the

glass slide manually (5-10 μm) with the *Z-Stepper Motors*. Once contact is made, retract immediately.

20| Ensure the cantilever is a larger distance from the glass slide than the bead diameter (*e.g.,* 200-300 μm), and move the *Sample Holder* until the cantilever is over the beads.

21| While focusing on the beads and making minor adjustments of the *Sample Holder* or *AFM head* position, slowly bring the tip of the cantilever into contact with a single bead and then retract the cantilever away from the slide (~200 μm).

Δ CRITICAL STEP The step sizes used to approach the bead should be small and selected prudently to avoid damaging the cantilever.

Δ CRITICAL STEP Proper attachment of the bead to the cantilever is vital. Select a single, isolated bead as nearby beads can interfere with the cantilever approach or damage the cantilever.

Δ CRITICAL STEP A short pause (5-10 s) after bead-tip contact can often improve adhesion, especially for large beads (>20 μm diameter).

22| Move the *AFM Head* to its maximum height position using the *Z-Stepper Motors* and switch off the laser. Remove the *AFM Head* and glass block cantilever holder.

23| Using forceps, carefully return the probe bead face up in the manufacturer's box.

24| Expose the opened manufacturer's box to the UV lamp for ~5-10 min to cure the glue. Steps 3-24 can be repeated multiple times to create many sphere-mounted cantilevers in a single session.

Δ CRITICAL STEP Although a single bead-mounted cantilever can be used to test multiple samples, probes can also be damaged during use and must be replaced. Having 5-10 bead-mounted probes at the ready will ensure an experimental session is not compromised by a lack of prepared cantilevers.

25| *Confirm bead attachment.* Place the manufacturer's box containing the cantilever(s) under the stereomicroscope, and adjust the focus until the cantilever is visible. There should be a single bead attached to the end of the cantilever, which should not be coated in glue or otherwise damaged. Proper bead attachment can also be determined by performing a single *F-D* on a clean glass slide (Steps 26-32, "Calibrating photodiode sensitivity"). *F-D* curve abnormalities suggest issues with bead attachment.

 PAUSE POINT Probes can be stored at room temperature (22 ºC) inside the manufacturer's box for up to 6 months.

Calibration of the cantilever ●TIMING ~ 10 min

26| *Calibrating the photodiode sensitivity (Steps 26-32).* Mount a cantilever onto the glass block cantilever holder using forceps and position it into the AFM head as described in Steps 4-6.

27| Place a clean glass slide in the *Sample Holder* and mount the *AFM Head* into its 3-leg position as described in Step 7.

28| Switch on the laser and then align the Laser and Photodiode (see also Steps 8-11). When using NanoWizard 4, follow Option A. When using the JPK CellHesion system, follow Option B.

(A) Initial calibration using JPK NanoWizard 4

i. The software's default settings are often suitable: *IGain*: 150 Hz, *PGain*: 0.0048, *Setpoint*: 0.3 V, and *Relative setpoint*: 0.4 V.

ii. The *Relative setpoint* may need to be increased to ensure the sensitivity can be calibrated properly.
iii. For soft cantilevers (0.01-0.06 N/m), *Feedback Control* parameters may also need to be decreased.
iv. The *Z-Length* may also need to be increased to ensure the bead fully detaches from the slide after indentation.

(B) Initial calibration using the JPK CellHesion system

i. The default *Feedback Control* parameters are often lower than those of the Nanowizard 4 (*IGain*: 5 Hz, *PGain*: 0.0002, *Relative Setpoint*: 0.2 V) and may need to be adjusted.
ii. The *Z-Length* may also need to be increased to ensure the bead fully detaches from the slide after indentation.

29| Use the *Z-Stepper Motor* to lower the cantilever towards the glass slide, but do not come in direct contact with it. Once the tip is near the glass slide, use the *Approach* function to execute an automatic approach to the glass slide.

Δ CRITICAL STEP Within the JPK software there are two types of *Approach Parameters*: (A) *Approach with feedback* and (B) *Approach with constant velocity*. Whilst both options use the same approach routine, we recommend using *Approach with constant velocity* for tips functionalized with beads. With both approach routines, baseline adjustments should be selected (*e.g., Baseline update at start* option) in the *Approach Parameters* window to account for any deviations in the baseline due to thermal effects or electrostatic interactions. The default *Approach Height* setting (7.5 μm) should be appropriate for most measurements.

Δ CRITICAL STEP When approaching the glass slide, always use the *Approach* function, which switches the instrument to software control of *Approach Height* and prevents the glass block and cantilever from colliding into the glass slide

Δ CRITICAL STEP Once the cantilever has approached the slide, make sure that it is stable (indicated in the *Laser Alignment* window).

30| Once approach is completed, click *RUN* to collect a *F-D* curve. This should be a force curve with a flat baseline and a smooth consistent indentation.

31| Open the *Calibration Manager* window and ensure contact-based calibration is selected. The sensitivity (nm/V) is calculated from the gradient of the *Extend* curve and is necessary to convert photodiode deflection into units of length. Select the linear portion of the *F-D* curve (selecting at least 50-100 nm of deflection). Accept the calculation of sensitivity and withdraw the cantilever at least 100 μm from the surface.

32| Repeat Steps 29-31 three times and take the average deflection sensitivity across the three measurements.

? TROUBLESHOOTING

33| *Measuring the cantilever spring constant (Steps 33-35).* Ensure the cantilever is retracted from the slide (>200 μm). In the *Calibration Manager* window, select the *Thermal Noise* tab (or *Spring constant* tab for CellHesion) and click *Run Thermal Noise* to measure thermal fluctuations in the cantilever. The resulting frequency spectrum should have a peak (first resonance) at the cantilever's expected resonance frequency (as indicated by the

manufacturer). The thermal noise method is dependent on temperature. The default setting of 25 °C can be changed under *Settings* in the calibration window to match the temperature of the room. If needed, the angle of the cantilever can also be adjusted here. For most JPK systems, the default setting of 10° (from the cantilever holder) will be correct. This does not need to be changed unless the cantilever is at a further angle from the chip.

34| Use the *Select Fit Range* button to fit a Lorentzian curve to the spectrum at the expected resonance frequency. This fitting will calculate the cantilever's spring constant (N/m).

35| Repeat Steps 33-34 three times to ensure consistency.

Δ CRITICAL STEP Calibration of the cantilever using the Thermal Noise Method[51,79] is essential to allow the instrument to convert the deflection of the cantilever in nm to force in N.

Δ CRITICAL STEP Many cantilever manufacturers provide an expected spring constant range. It is advisable to check that the calculated spring constant falls within the manufacturer's expected range.

Δ CRITICAL STEP The cantilever can be calibrated either pre- or post-bead attachment[80]. The thermal noise method assumes the mass of the tip is negligible compared to the mass of the cantilever. However, it has been reported that large glass beads (>10 μm diameter on 200 μm silicon nitride beam cantilevers) can impact the cantilever's resonance frequency[81]. Thus, for large beads, and particularly on beam cantilevers, it is advisable to measure the cantilever's spring constant before attaching the bead, as it can interfere with the Thermal Noise Method. If calibration is done pre-bead attachment, carry out Steps 26-35 before attaching a bead. The spring constant value can then be entered into the spring constant box in the *Calibration Manager* window instead of calculating it using the Thermal Noise Method after attachment. For smaller beads, once the bead is attached, it's advisable to measure the spring constant again to ensure it has not changed. Regardless of whether the spring constant is calculated pre- or post-bead attachment, the sensitivity of the photodiode (deflection sensitivity, Steps 26-32) should be measured at the start of every experiment.

Δ CRITICAL STEP When calibrating the cantilever using the Thermal Noise Method, it is also possible to apply a correction factor in the *Calibration window*, which takes into account how the actual cantilever bends compared to what is detected through the photodiode (*e.g.,* calibrated through the *deflection sensitivity)*. For rectangular (beam) cantilevers, for example, a correction corresponding to the first resonance peak (eigenmode) is often applied[45,82].

Δ CRITICAL STEP Once the tip is calibrated, the laser position should not be moved. If the laser position on the cantilever is moved for any reason (*e.g.,* tip being knocked), re-calibrate the tip. The photodiode position (*Laser Alignment*) and *Mirror* can be adjusted post-tip calibration.

? TROUBLESHOOTING

Stabilization of the cantilever in liquid ●TIMING ~ 1 h

36| *Re-calibrating the photodiode sensitivity in liquid (Steps 36-43).* To account for changes in refractive indices when moving from air to liquid, the photodiode sensitivity needs to be re-calibrated. Ensure that the *AFM Head* is at its maximum *Z-position height* using the *Z-Stepper Motor.*

37| Switch off the laser, remove the *AFM Head* and carefully add PBS (or the buffer the sample is immersed within, *e.g.,* cell culture medium) dropwise to the end of the glass cantilever holder using a pipette, encapsulating the cantilever in a drop of solution.
38| Using a hydrophobic immunohistochemistry PAP pen, draw a small circle onto a clean glass slide and just fill with PBS (or appropriate buffer, ~200-500 µL).
39| Place the slide in the *Sample Holder* and position the *AFM Head*/tip above the solution.
40| Using the *Z-Stepper Motor*, carefully lower the tip into the solution so that the drop encapsulating the cantilever meets the solution on the glass slide (fully submerging the cantilever). Do not make contact with the glass slide.
41| Switch on the laser, re-adjust the *Mirror* (*Mirror adjustment screws*) to compensate for the change in the refractive index. Ensure that the cantilever is stable by checking the *Laser Alignment* window. If necessary, use the *Detector adjustment screws* to align the cantilever to the centre of the *Detector.* Once centred, gently turn the *Mirror adjustment screw* to optimize the angle of the *Mirror* so that the *Sum signal* is maximized.
Δ CRITICAL STEP It may take 10-30 min for the vertical deflection signal (indicated in the *Laser Alignment* window) to stabilize.
42| Once vertical deflection signal stabilizes, repeat Steps 26-32 to calibrate the sensitivity of the cantilever in liquid.
43| Leave the cantilever in the PBS until Step 44 has been completed before proceeding to Steps 45-50. Never immerse the *Sample Stage* or *Sample Holder* in liquid and do not spill solutions on the microscope optics.
Δ CRITICAL STEP The spring constant of the cantilever (measured in air) does not need to be re-measured in liquid.
Δ CRITICAL STEP Ensure that the space between the cantilever and the glass block is completely immersed in PBS/buffer. If the cantilever is not immersed, it can bend excessively and become damaged as it penetrates the liquid.
Δ CRITICAL STEP If performing measurements on live cultures, the cantilever must be calibrated in the same solution the samples are within and at testing temperature (*e.g.,* cell culture medium without serum).
Δ CRITICAL STEP If bubbles or debris are visible near the cantilever, they should be removed as they may interfere with measurements. Move the *Z-Stepper Motor* up to the maximum Z-position, turn off the laser, remove the *AFM Head*, and add PBS dropwise to the glass cantilever holder to wash away debris. Use a precision wipe to adsorb excess of liquid, while making sure not to touch the cantilever.

Mounting the sample ●TIMING ~ 30 min
44| Mount the sample. For free-floating 3D hydrogels, follow Option A. For 2D material surfaces attached to glass slides, follow Option B. For 3D hydrogels adherent to plastic surfaces, follow Option C. For 2D hydrogels or material surfaces attached to glass/plastic slides/coverslips, follow Option D.
(A) ***Free-floating 3D hydrogels (e.g., HA hydrogels, collagen gels).***
(i) Transfer hydrogels to a 60 mm dish (wall height ≤6 mm) using a small spatula and immobilize it by carefully balancing two 13 mm coverslips, each on opposite ends of the hydrogel. The

hydrogel surface should remain free between the coverslips, but the load they apply should be sufficient to hold the hydrogel in place, avoiding the need to glue the hydrogel to the petri-dish.

(ii) Use super glue to attach the coverslips to the underlying 60 mm dish, being careful to not place glue on the hydrogel itself. Wait 2 min to allow the glue to set.

(iii) Gently pipette 4.5 mL PBS into the dish, aspirate it and then add 4.5 mL of fresh PBS (or appropriate buffer) to the dish (Fig. 3c).

Δ CRITICAL STEP Shallow dishes (maximum height of 6 mm) are essential to allow the cantilever to approach the sample surface. Taller dishes may impede the downward movement of the AFM Head.

Δ CRITICAL STEP Although it may be possible to directly glue free-floating 3D hydrogels to culture dishes, in our hands, this is often not successful. Moreover, for inverted microscope setups, glue can interfere with visualizing the cantilever and the sample.

Δ CRITICAL STEP Use sterile, high quality PBS or other appropriate medium, and fresh, sterile dishes for each sample. Wear clean gloves when mounting the sample.

(B) ***2D material surfaces attached to glass slides (e.g., PA).***

(i) Using a PAP pen, draw a large circle round the surface/hydrogel.

(ii) Add PBS or cell culture medium into the circle, submerging the sample in a bubble.

Δ CRITICAL STEP Use sterile, high quality PBS or other appropriate medium, and fresh, sterile dishes for each sample. Wear clean gloves when mounting the sample.

(C) ***3D hydrogels adherent to plastic surfaces (e.g., peptide-modified PEG hydrogels or Matrigel).***

(i) Hydrogels that adhere to tissue culture plastic and do not free-float in liquid can often be formed in a low-walled 60 mm dish and measurements performed directly in the dish (Fig. 3d). Prior to making AFM measurements, replace cell culture medium with CO_2-independent serum-free media.

Δ CRITICAL STEP Shallow dishes (maximum height of 6 mm) are essential to allow the cantilever to approach the sample surface. Taller dishes may impede the downward movement of the AFM Head.

Δ CRITICAL STEP Use sterile, high quality PBS or other appropriate medium, and fresh, sterile dishes for each sample. Wear clean gloves when mounting the sample.

(D) ***2D hydrogels or material surfaces attached to glass/plastic slides/coverslips (e.g., PA or PDMS).***

(i) Transfer a 2D hydrogel/surface attached to a coverslip to a 60 mm dish using forceps.

(ii) Immobilize the coverslip by gluing it to the bottom of the dish using a small amount of superglue. Wait 2 min to allow the glue to dry. Alternative immobilization strategies have also been reported to be effective[27,32].

(iii) Gently pipette 4.5 mL PBS into the dish, aspirate it and then add 4.5 mL of fresh PBS (or appropriate buffer) to the dish.

Δ CRITICAL STEP Shallow dishes (maximum height of 6 mm) are essential to allow the cantilever to approach the sample surface. Taller dishes may impede the downward movement of the *AFM Head.*

Δ CRITICAL STEP Use sterile, high quality PBS or other appropriate medium, and fresh, sterile dishes for each sample. Wear clean gloves when mounting the sample.

45| *Placing the sample on the instrument (Steps 45-50).* Raise the cantilever to its maximum height using the *Z-Stepper Motor*.
46| Switch off the laser and remove the *AFM Head*.
47| Adhere the dish containing the hydrogel sample to the *Sample Holder* on the stage using plasticine.
Δ CRITICAL STEP For free-floating 3D hydrogels held in place with 13 mm coverslips, orient the sample such that the cantilever approaches the sample between the coverslips rather than over them.
48| Put the *AFM Head* back on the stage into its 3-leg position.
49| Use the *Z-Stepper Motor* to bring the cantilever into the dish/slide, fully immersing it.
50| Wait at least 20 min to allow the cantilever to stabilize in the liquid.

Carrying out *F-D* measurements ●TIMING 1-2 h
51| *Identifying appropriate parameters (Steps 51-57)*. Indentation parameters should be set in the *Spectroscopy Control* box.
52| Depending on the expected sample stiffness, the applied force will vary. For hydrogels with an expected *E* in the range of 0.3-100 kPa, set the *Relative Setpoint* in the range of 2-30 nN. It is advisable to start with a lower *Relative Setpoint* and increase it until a suitable *F-D* is obtained. For higher *Relative Setpoints*, the indentation depth will increase. Many mechanical models for calculating *E* assume that the indentation depth is small compared to the radius of the colloidal probe. Therefore, indentation depth should not exceed more than ~1/3 of the bead radius. For larger beads, it is possible to use a higher *Relative Setpoint.*
53| Adjust the *Extend Speed* depending on sample properties. Faster speeds reduce acquisition time, but can lead to drag on the tip (resulting in a baseline that is not flat). For soft hydrogels, set *Extend Speed* in the range of 2-15 μm/s. For AFM instruments on which the scan rate is shown in Hz, the tip speed can be calculated by multiplying the total Z-length (Ramp size) by the force (scan) rate.
54| Softer hydrogels may require a longer *Z-length* than stiffer hydrogels to ensure the tip properly detaches following indentation. Set *Z-length* in the range of ~10-14 μm.
55| For most measurements, enable *Z-closed loop* and set the Extend/Retract rate to *Constant Speed* to ensure a consistent loading/unloading rate.
56| For measurements in liquid, lower the *Sample Rate* to reduce noise (from the default 2048 to 1024, *e.g.*); however, care must be taken to ensure the number of data points collected is sufficiently high enough to detect all features within the *F-D* curve.
57| If necessary, alter *Approach* parameters/*Feedback Control* depending on the samples' properties (*e.g.,* stiffer materials may require a higher *Setpoint*). *Approach Height* can also be adjusted. In particular, for the NanoWizards 1 and 4, *Approach Height* may need to be lowered if the desired Z-length is more than 7.5 μm.
Δ CRITICAL STEP Once ideal conditions have been identified, *F-D* measurements should be performed using identical parameters. In particular, *Relative setpoint* and *Extend speed* should remain constant so that the measurements can be compared across experimental conditions.

? TROUBLESHOOTING

58| *Approaching the hydrogel surface (Steps 58-62)*. Adjust the microscope to focus on the top surface of the sample.
59| Identify the area you intend to probe by moving the *Stage* using *Screws* to move the *Sample Holder* (or use the Joystick, if using a motorized stage). For samples immobilized with 13 mm coverslips, it is important to avoid the areas close to the coverslips.
60| Switch on the laser. Make sure the laser is aligned on the cantilever and photodetector as described in Steps 8-11.
Δ CRITICAL STEP If using a motorized XY *Stage*, make sure to click *Centre Stage* at the start of the experiment to reset the *Stage* to its original (0,0) x,y position. Make sure the objectives are well clear of the *Stage* before doing this.
61| Use the *Z-Stepper Motor* to bring the cantilever towards the surface of the sample (using 100-200 μm steps), checking that the tip is stable by watching for movement in the *Laser Alignment* window. Stop once the shadow of the cantilever is visible in the camera image.
62| Once close to the sample surface, use the *Approach* function to bring the cantilever to the surface of the gel. As mentioned in Step 29, *Approach with constant velocity* is preferred for cantilevers functionalized with beads. In the Approach parameters window ensure *Baseline Adjust* is enabled by selecting either *Baseline update at start* or *Dynamic baseline update.*
? TROUBLESHOOTING

63| Collect F-D measurements. For manual collection, follow Option A. For automatic collection of F-D maps, follow Option B.
(A) *Collecting F-D measurements manually*.
(i) Before starting measurements, ensure the *Autosave* function is enabled and in the saving settings the *Height*, *Height (measured)*, and *Vertical Deflection* channels are selected for both the *Extend* and *Retract* curve.
(ii) Click *RUN* to perform a single *F-D* curve.
(iii) Retract the probe ~100-200 μm from the surface.
(iv) Select another area of the sample by using the *Screws* to move the *Sample Holder* (or use the Joystick, if using a motorized stage) or *Screws* to move the *AFM Head,* from the original measurement point and repeat the process again to perform another *F-D* curve. Repeat Steps i-iv across the sample surface and on replicate samples.
Δ CRITICAL STEP Variations in the temperature of the experimental setup can impact reproducibility. Ensure that measurements are always made at constant temperature.
Δ CRITICAL STEP Measurements should not be performed close to the edge of a sample.
Δ CRITICAL STEP Hydrogels should be kept hydrated during preparation, mounting and measurements.
Δ CRITICAL STEP Environmental disturbances (loud noises, ventilation systems, passing colleagues, *etc.*) may add noise to the data. Avoiding such circumstances and a good isolation table or acoustic hood should ensure stable measurements.

? TROUBLESHOOTING

(B) ***Collecting automatic F-D maps.***

(i) Select the *Spectroscopy Pattern Manager* in *Force spectroscopy* mode, or *the Data Viewer* window in *Force mapping*, and choose the map size and the number of desired data points (*e.g.,* 100 µm x 100 µm, 10 x 10 points).

(ii) For *Force Spectroscopy* maps, ensure that *Go through XY position list* is selected in the *Force Scan repetitions* window. The *Force Scan repetitions* window also allows for multiple curves for a single point to be collected.

(iii) Approach the cantilever to the surface of the sample in the area of interest.

(iv) Make sure the *AFM Head* is at the starting position (Position 0), select *Autosave*, and click *RUN*. This will prompt the *AFM Head* to move through all the points marked on the grid (Fig. 3d).

(v) Repeat Steps i-v to collect maps in different areas of the sample surface (*e.g.*, 6 different areas, generating a total of 600 measurements).

Δ CRITICAL STEP It is often advisable to make a few manual measurements before collecting *F-D* curves automatically in grids. This ensures that parameters/settings are correct and sufficient to collect optimal *F-D* curves on an area of interest.

Δ CRITICAL STEP For the CellHesion instrument, the coordinates of the stage (X/Y) need to be input into *X Offset* and *Y Offset* in the *Grid manager* or *Data viewer* to ensure the grid map is placed on the correct area. Failure to do this can result in large, unexpected movements of the stage, which can damage the tip.

Δ CRITICAL STEP Variations in the temperature of the experimental setup can impact reproducibility. Ensure that measurements are always made at constant temperature.

Δ CRITICAL STEP Measurements should not be performed close to the edge of a sample.

Δ CRITICAL STEP Hydrogels should be kept hydrated during preparation, mounting and measurements.

Δ CRITICAL STEP If correlating force maps with optical images (Step 88D), take snapshot photos of the cantilever at the top left and bottom right positions of the force map/grid.

Δ CRITICAL STEP Environmental disturbances (loud noises, ventilation systems, passing colleagues, *etc.*) may add noise to the data. Avoiding such circumstances and a good isolation table or acoustic hood should ensure stable measurements.

? TROUBLESHOOTING

64| *Swapping samples (Steps 64-68).* To swap samples, retract the cantilever at least 500 µm, moving it out of the PBS/medium.

65| Switch off the laser and remove the *AFM Head.*

66| Follow Steps 36-43 to maintain the cantilever stabilized in liquid, either on a glass slide or in a petri dish filled with the testing solution, until the next sample is ready.

67| Repeat Step 44 to mount a new sample.

68| Repeat Steps 45-63 to carry out *F-D* measurements on additional samples.

Switching off the microscope ●TIMING ~ 10 min

69| Raise the *AFM Head* to its maximum height position using the *Z-Stepper Motors*.

70| Switch off the laser and remove the *AFM Head*.

71| Blot excess liquid from the glass block cantilever holder and carefully remove it after unlocking it.
72| To avoid salt crystal formation on the cantilever, wash with sterile water and allow to dry.
73| Using forceps with plastic tips, remove the cantilever and place it back in the manufacturer's box.
74| Wash the glass block cantilever holder with distilled water and ethanol, dry with precision wipes, and place it in its support.
75| Close the Micro-Manager software (if using) and the JPK SPM software.
76| Switch off the computer and screens, camera, fluorescence (if used), microscope light and main power.

 PAUSE POINT *F-D* curves can be saved and processed at a later date.

***F-D* curve analysis** ●TIMING (~600 force curves) ~ 1 h
77| *F-D curves pre-processing (Steps 77-85).* Prior to calculating *E*, use the JPK data processing software to pre-process *F-D* curves using the series of simple steps given below (but which are also explained in detail in the data processing manual):
78| Using *Batch Processing,* open all *F-D* curves.
79| Click *Re(Calibrate)* and check that the correct *Sensitivity* and *Spring constant* values have been applied (as calculated/measured in Steps 26-43).
80| *Smooth* the data using the Gaussian function, making sure not to have the width too high, which might change the curve's shape drastically.
81| Carry out a *Baseline offset* correction (Baseline Subtraction to the extend curve), and if needed correct for any tilt (*Offset and Tilt*) to ensure the baselines are flat.
82| Calculate *Tip-Sample Separation*.
Δ CRITICAL STEP Calculating *Tip-Sample Separation* is crucial to correct for cantilever bending and will shift the x-axis of the *F-D* curve from *Height measured* to *Vertical tip position* (or *Tip-Sample Separation,* depending on software version).
83| If applying the Hertz model using the JPK software, skip to Step 86 Option (A), otherwise proceed to Step 84.
84| Move through *F-D* curves (*Keep),* discarding (*Discard) F-D* curves with abnormalities.
Δ CRITICAL STEP Example *F-D curves* from successful indentations are shown in Fig. 5a. For many 2D culture surfaces and hydrogels, the retraction curve will have a constant slope. *F-D* curves can also appear noisy and the retract curve's slope may vary (Fig. 5a). Sometimes *F-D* curves can have sudden, large shifts caused by acoustic noise or mechanical interference. Interference with the cantilever and debris in the solution may similarly cause unwanted cantilever deflection. Such *F-D* curves should be discarded.
Δ CRITICAL STEP For hydrated samples like hydrogels, expect that a large fraction of *F-D* curves will be discarded.
85| Save pre-processed *F-D* curves into a new folder.

86| Calculate E from processed F-D curves. For using the Hertz model, follow Option A. For using the Oliver-Pharr model, follow Option B.
(A) *Hertz model* (*spherical probe*).

(i) Select *Elasticity Fit* in the shortcut icons, making sure that the *Hertz/Sneddon* option is selected as the model type in the fit parameters. Set tip shape to sphere and tip radius to match that of the bead.
(ii) Using the *fit data* icon, fit the model to the *Extend* curve, ensuring that the model curve aligns with the *F-D* curve. Discard *F-D* curves that the model does fit properly or if they have any abnormalities.
(iii) Once all curves are processed, *Save Final Data.* This will generate an Excel file containing all values of *E*.
(B) *Oliver-Pharr model* (*spherical probe*).
(i) Using JPK's data processing software convert accepted pre-processed *F-D* curves into .txt files: open the folder containing the pre-processed curves in the *F-D* curve batch processing menu and under the save tab, select to export the curves as .txt with just the *Retract* box under *Segments* selected. Under *Header* make sure *Full Settings* is selected*, Force* is selected under *Output unit for Vertical Deflection,* and all the boxes are ticked under *Channels*.
(ii) Repeat the Step (i), but for the *Extend* curves, saving just the extend portion.
(iii) Rename the retract and extend .txt files (retract1, retract2, etc. and extend1, extend2, etc).
(iv) Open Matlab, ensuring that the scripts (Oliver_and_Pharr_model.m and Contact_point.m; see https://github.com/eileengentleman/AFM-code) are running from the same location as the folder which contains the pre-processed *F-D* curves.
Δ CRITICAL STEP See Supplementary Note 1 for a description of the theoretical basis for Oliver-Pharr-based Matlab code and further details on how to operate the code.
(v) In the Matlab script (Oliver_and_Pharr_model.m), adjust bead radius (*R*) and *Poisson's ratio* (*v*) in accordance with the experimental set-up. Set *number_curves* to the number of force curves that are to be analyzed, and make sure that *startingrow* corresponds to the row in which the data starts in the .txt file (this should be 79). The percentage of the retract curve used to calculate the slope can be changed (*Percentage*); however, 25% taken at the upper portion of the retract curve (close to the indentation), is appropriate for most force curves. Ensure that the *Folder* name matches that of the folder containing the retract/extend .txt files.
(vi) Click *RUN* on the Matlab script. This will process all selected *F-D* curves and generate plots for the Full *Extend* curve, Full *Retract* curve, *Retract curve (Fmax – Fmin),* a histogram of *Indentation depth* and *Retract length (Fmax – Fmin),* and the sectioned *Retract* curve, which is used to calculate *E*. It will also generate two excel files, one listing the Reduced Modulus and the other *E*.
87| *(Optional) Consider removing outliers.* Using GraphPad Prism version 8 (GraphPad Software, USA), prepare a *Column Table* to enter values for *E* stacked into columns. Use the menu *Analyze* to identify outliers with the ROUT method, setting Q = 1%. This allows just 1% of identified outliers to be false. This process generates 3 tables: *Clean data, Outliers,* and *Summary*. Use *Clean data* in the following steps.

Generating data plots ●TIMING ~ 6 h, depending on the number of *F-D* curves
88| *Plotting E.* Using a software package such as GraphPad Prism version 8 (GraphPad Software) create plots for *E*. Different plot types can be selected in the graph type menu:
(A) Plot data as *box plots and whiskers*

(i) Plot the data as box plots and whiskers with the median (central line), 1st and 3rd quartiles (bounds of box), and high and low values (whiskers) (Fig. 5b).

(B) Plot data as *histograms*.

(i) Plot histograms in a software package such as OriginPro software.

(ii) Adjust bin sizes to the range of values obtained for each sample.

(iii) Use *Frequency Count* to define the minimum, maximum, increment and bin centre.

Δ CRITICAL STEP If datasets have different numbers of *F-D* curves, plot Frequency (%) instead of absolute values. For effective comparisons, bin sizes should be the same between groups.

(iii) In the *Analyze* menu, choose *fit a single peak* or *fit multiple peaks*. Define the peak centre using the Gaussian function. This step will calculate the peak centre, standard error and standard deviation

(iv) Overlay fitted normal distributions on histograms (Fig. 5b).

(C) Plot data as *dot plots*

(i) Plot the data as dot plots showing all measurements, with a horizontal line indicating the median (Fig. 5c).

(D) Plot maps of *E* as *heatmaps*.

(i) Batch process *F-D* maps as described in Steps 77-86, noting the position of any *F-D* curves that are discarded.

(ii) Using GraphPad Prism, create a grouped table matching the *F-D* map dimensions.

(iii) Enter values of *E* into the table ensuring that each value is placed in its corresponding position. For curves that were discarded, leave that corresponding cell blank in the table.

(iv) Under graph type, select *heatmap* and choose a colour scheme.

(v) To align a *heatmap* with an optical image, use snapshots (Step 63B) taken of the cantilever to match the top left and bottom right positions on the optical image to corresponding positions on the heatmap of *E* (Fig. 5d).

(E) Plot data as *violin plots*

(i) Plot the data as violin plots to show the frequency distribution (Fig. 5e).

89| *Statistical analyses of E*. Choice of statistical test will depend on the distribution of the data. Using GraphPad Prism, prepare a *Column Table* to enter values of *E, stacked into columns*. Determine if datasets are normally distributed using a Shapiro-Wilk normality test. In the *Analyze* menu, choose *Column Analyses*, and choose *Normality and Lognormality Tests.* Click *Shapiro-Wilk normality test*. For normally distributed datasets, follow Option A. For non-normally distributed datasets, follow Option B.

(A) *Normally distributed datasets.*

(i) In the *Analyze* menu, choose *Column Analyses*, and choose the data sets that are to be compared.

(ii) If comparing two groups, choose *t tests* (*and nonparametric tests),* select an *unpaired experimental design*, *assume Gaussian distributions* and *use parametric test*. In *Options* tab calculate *p value two-tailed* with *95% confidence level (p < 0.05).* The resulting *p* value indicates if the means are significantly different from one another.

(iii) If comparing 3 or more groups, choose *One-way ANOVA* (*and nonparametric test*), select *no matching or pairing experimental design* and *assume Gaussian distributions.* In the *Multiple*

Comparisons tab select *compare the mean rank of each column with the mean rank of every other column.* In the *Options* tab select *Tukey post-hoc test.* Select *report multiplicity adjusted p value for each comparison.* Set the *family-wise significance and confidence level* to 0.05. The resulting *p* value indicates if the means are significantly different from one another.

(B) *Non-normally distributed datasets.*

(i) In the *Analyze* menu, choose *Column Analyses*, and choose the data sets that are to be compared.

(ii) If comparing the median value between two groups, choose *t tests* (*and nonparametric tests),* and select an *unpaired* experimental design and *nonparametric test.* Choose *Mann-Whitney test (two-tailed).* Alternatively, conduct a non-parametric *Kolmogorov-Smirnov* test to compare the distribution of the two data sets (Fig. 5e).

(iii) If comparing more than 2 groups, choose *One-way ANOVA (and nonparametric)*, and select *no matching or pairing* experimental design, and *nonparametric test Kruskal-Wallis*. Then choose *multiple comparisons test Dunn's* to *compare the mean rank of each column with the mean rank of every other column*. The *family-wise significance and confidence level* should be 0.05.

90| *Statistical analyses of distributions of E.* In addition to comparing *E* between different groups, comparisons on the distributions of values of *E* may be of interest (*e.g.,* Fig. 5b) and can be evaluated using one or more of the following tests:

(A) A Mantel-Haenszel linear-by-linear association Chi-square test

(i) Perform a Mantel-Haenszel linear-by-linear association Chi-square test for trend (χ^2) (degrees of freedom = 1) can be used to test if the distributions are significantly different from one another.

(B) A non-parametric Goodman and Kruskal's gamma (γ) test

CRITICAL: This option should be followed after completing the Mantel-Haenszel linear-by-linear association Chi-square test described in Option A.

(i) Perform a non-parametric Goodman and Kruskal's gamma test to measure the strength of association that exists between any two comparisons. Low values for association indicate that two distributions are highly similar, while higher values are evidence of a stronger association and indicate that the distributions are different: none (0.00 ± 0.01), moderate association (± 0.10 – 0.29), strong association (± 0.30 – 0.99).

(C) Standardized residuals (*SR*)

CRITICAL Standard residuals highlight the most significant areas of the histograms that contributed to differences. All three statistical analyses can be performed using IBM® SPSS® statistics version V23. To calculate these, in the *Data View* window:

(i) Input all values of *E* in the 1st column.

(ii) In the 2nd column, define which sample each value of *E* in the 1st column belongs to (*e.g.*, label "1" for sample 1 and label "2" for sample 2).

(iii) In the 3rd column, categorize the values of *E* in the 1st column (*Input Variable*) in intervals of values (*Output Variable*). The last step will divide all values of *E* from the samples in intervals (bins): *e.g., (Range, LOWEST through value 500=1), (Range: 501 through 1000 = 2), etc..* Once finished, accept to *Change*.

(iv) Use menu *Transform* and *recode into different variables (ordinal).*

(v) (Optional) In the 2nd and 3rd columns, sample and intervals can be relabelled to allow easier interpretation of the statistical analysis: *e.g.,* in 2nd column, "1" can be relabelled "acellular hydrogel", and "2" "cell-laden hydrogel", and in 3rd column, intervals of values can be relabelled (*e.g.,* 1 = "<500", 2 = "501-1000", etc.).
(vi) Select the menu *Analyze*, *Descriptive Statistics*, *Crosstabs* and highlight the dependent variable (in this example, 2nd column) and the independent variable (in this example, 3rd column). Select *Statistics* as *chi-square*, *Residuals* as *standardized* and *gamma* to evaluate the power. Click on *Cells counts observed % column* and select *Round cell counts*. Then click *Continue* and *OK*.

? TROUBLESHOOTING
Troubleshooting advice can be found in **Table 1.**

TABLE 1 | Troubleshooting table

Steps	Problem	Possible reason	Solution
9	Failure to align laser on cantilever	Cantilever is not mounted in the correct position.	Remove the cantilever, clean the prism of the glass holder and mount the cantilever again. The cantilever must be mounted centrally, between the grooves.
		Defective cantilever.	Excess glue may have been placed on the cantilever or the bead not attached in the appropriate position. Try again with a new cantilever.
11	Failure to align laser with detector	Cantilever is not mounted in the correct position, is damaged or dirty.	Remount the cantilever. If unsuccessful, try again with a new cantilever. Ensure that the screws holding the tip in place are not fastened too tightly.
		Cantilever glass holder is dirty or scratched.	Remove the cantilever, clean the polished glass sides of the cantilever holder, and make sure it is not scratched.
		Laser is not properly aligned on the cantilever.	Reposition the laser on the cantilever. It should be at the very end of the cantilever tip. Increasing the light intensity of the microscope can make the

			laser dot smaller, making it easier to position.
		Detector adjustment screws cannot be turned farther.	Repeat Steps 8-11. Do not overtighten the *Detector adjustment screws*, as this will damage the AFM. Ensure the *Mirror* is also aligned correctly.
30	*F-D* curves have a sinusoidal wave pattern in the baseline.	Laser photons trapped between the sample surface and the underside of the cantilever.	Retract the cantilever and adjust the *Laser adjustment screws* to ensure that the laser spot is located at the center/end of the cantilever rather than on its edge.
31	Unsuccessful calibration of bead-mounted cantilever.	Static interactions between the bead and the glass slide.	If the cantilever fails to approach the slide, increase *Feedback Control* and *Setpoint Force*. To ensure proper detachment of cantilever from the slide after indentation increase *Z-length* and decrease *Approach Height*. If vertical position (indicated in the *Laser Alignment* window) drifts during approach, halt the approach and recentre the laser by re-aligning the photodiode. Alternatively, use a sapphire calibrating disk (*e.g.*, SAPPHIRE-12M, Bruker) instead of a glass slide, which will reduce static interactions.
		Bead is too large or cantilever spring constant calculated incorrectly with bead attached.	The attached bead can shift the cantilever's resonance frequency. If there is no clear peak at the expected resonance frequency, measure the cantilever's spring constant before attaching the bead.
60	Unstable vertical or	Vertical and lateral deflection drift while the	Allow the cantilever to stabilize immersed in

	lateral deflection of the laser.	cantilever is stabilizing. Cantilever holder clip/spring is loose.	appropriate buffer for longer before making measurements (Steps 36-43). Make sure there are also no air bubbles stuck to the cantilever or cantilever holder. Re-tighten or replace the spring (if necessary).
		Cantilever is dirty or defective.	Use an optical microscopic to visually determine if the cantilever is clean. Retract the cantilever. Remove the *AFM Head*. Rinse the cantilever with PBS by adding it dropwise. Use precision wipes to absorb excess PBS or replace the cantilever.
		The cantilever is sensitive to environmental effects.	Ensure that the environment is free from loud machine noises, disturbances from ventilation systems, passing colleagues, *etc*.
		The coating on the cantilever is compromised.	Some silicon cantilevers have an aluminium back coating that can corrode over time. For liquid measurements, use either uncoated silicon tips or gold-coated silicon nitride tips.
62	Unsuccessful approach.	The *Feedback Control* is either too slow or too sensitive and not searching the full Z-range.	Increase the *Setpoint* or *Approach velocity*. Ensure that the cantilever is not too far away from the sample before approaching. If the feedback is too sensitive (causing oscillations in the vertical deflection and a ringing sound) decrease the feedback by lowering either of the gains (*IGain* or *PGain*) and/or the *Setpoint.* A successful approach requires a setpoint that is high enough to detect the sample

			surface, but not so high that the probe presses deeply into the hydrogel. Upon approaching the gel surface, pause for 5-10 s to ensure that the Z-height is stable (Indicated in the *Z-piezo display menu*). If unstable, retract and re-adjust approach parameters.
		Sample is unstable (*e.g.,* swelling) or otherwise changing morphologically.	Ensure the sample is stable or wait for the sample to equilibrate.
63	Noisy *F-D* curves (*e.g.* high frequency or sinusoidal)	*F-D* curve sampling rate is too high.	Lower the *Sample Rate* (*e.g.,* ~ 1024).
		Vibrations or electrical interference.	If not sufficiently isolated, vibrations from nearby equipment can result in high frequency noise in *F-D* curves. Check that the air table is floating correctly. For electrical noise, check that electrical equipment is linked to a universal power supply and/or apply an electric noise filter.
63	*F-D* curves have non-standard/ irregular shapes (see Fig. 5a)	Contact time and/or the applied force are not appropriate.	Before adjusting force-spectroscopy settings, ensure the approach is consistently successful. Ensure that the *Relative setpoint* is appropriate. The probe should deform the hydrogel surface, but should not indent the gel by more than 1/3 bead radius. If both the approach and *Relative setpoint* are unproblematic, change the feedback settings one parameter at a time and try again.

		Oversampling of an area.	Ensure that the area of interest has not been oversampled. Repeated measurements at the same position or measurements close together in quick succession can impact *F-D* curves, particularly for materials that do not behave purely elastically. For measurements in maps, ensure the spacing is appropriate for the bead size to not oversample particular areas.
		Contaminated measurement solution.	Dust and debris in the solution can impact *F-D* curves. This is often the case if jumps in the *F-D* curve are evident before the contact point. Change the solution with fresh clean solution.
		The cantilever is dirty or defective.	Use an optical microscope to visually determine if the cantilever is clean and free from air bubbles. Adhesion on the *Retract* curve often indicates contamination on the bead. Retract the cantilever and remove the *AFM Head*. Rinse the cantilever with PBS by adding it dropwise. Use precision wipes to absorb excess PBS or replace the cantilever.
		Approach was not successful because measurements were made too close to the sample edge and/or irregular features on the sample surface precluded the cantilever reaching the sample surface.	Move the cantilever to another area of the surface of the sample to avoid debris in the medium or irregularities on the sample surface. The surface of 3D hydrogels can have a concave shape. Care should be taken to ensure the cantilever holder does not hit the sample before the tip makes contact.
		Extend Speed is too	Lower the *Extend Speed* (<15

		high.	μm/s).
		Sample temperature is inconsistent.	Fluctuations in sample temperature can result in uneven baselines. Minimize fluctuations in room temperature or use a plate heater to maintain a constant temperature.
		Bead is not attached properly or not at the cantilever tip.	Small deviations at the bead-cantilever interface or defects in the gluing can cause noisy *F-D* curves. Change the cantilever.
		Bead adheres to the sample.	If possible, perform measurements in ethanol or detergent solution to reduce adhesion[32].
		Sample moves during measurement	Ensure the sample is fixed in position and does not move. Repeat Step 44 to remount the sample.
86	Calculations yield unexpected values for *E*.	*F-D* curves not collected properly.	Carry out the protocol to measure the *E* of a reference material (*e.g.,* Petrisoft 35, Matrigen) and adjust *F-D* curve collection parameters as necessary.
		Poor *F-D* curve rejection criteria.	Only *F-D* curves that have a smooth *Extend* curve should be accepted. If using the Oliver-Pharr model to fit to the *Retract* curve, make sure to reject curves in which tip/sample interactions are strong (large difference in the slope of the extend and retract curves).
		Cantilever was not calibrated correctly or damaged during measurements.	Recalibrate the photodiode sensitivity after collecting *F-D* curves to ensure that it has not changed. Check that the calculated spring constant is within the manufacturer's expected range.

		Incorrect Fmin identified in Oliver-Pharr script.	If strong tip-sample adhesion is evident on the *Retract* curve, decrease the *Percentage* of the retract curve used in the Matlab code.
		Incorrect contact point identified in Oliver-Pharr script.	Visually examine the output of the code (indentation depth histogram) to determine if the contact point has been calculated (Contact_Point) correctly. Large variation in indentation depths also suggest incorrect contact point fitting.
		Incorrect model applied to calculate *E*.	If considerable tip-sample adhesion is evident on the *Retract* curve, consider applying an alternative model, such as the JKR.

TIMING

Steps 1-2, Switch on the microscope: ~ 5 min
Steps 3-7, Mounting the cantilever: ~ 15 min
Steps 8-11, Alignment of the laser and photodiode: ~ 5 min
Steps 12-25, Mounting a bead on a cantilever ~ 40 min
Steps 26-35, Calibration of the cantilever: ~ 10 min
Steps 36-43, Stabilization of the cantilever in liquid: ~ 1 h
Steps 44-50, Mounting the sample: ~ 30 min
Steps 51-68, Carrying out *F-D* measurements: ~ 1-2 h
Steps 69-76, Switch off the microscope ~ 10 min
Steps 77-87, *F-D* curve analysis (~600 force curves) ~ 1 h
Step 88-90, Generating data plots: ~ 6 h, depending on the number of *F-D* curves

ANTICIPATED RESULTS

The main output of this protocol will be *F-D* curves that will allow for calculation of *E*. When testing soft hydrated samples, and particularly samples containing live cell cultures, an array of *F-D* curve shapes will be generated. We show example *F-D* curves collected on PEG-based hydrogels using a 10 μm glass bead mounted onto a 0.12 N/m cantilever in Fig. 5a. Accepted force curves have a smooth extend curve and a retract curve with a constant slope. *F-D* curves that are discarded in our protocol display excessive noise, show an unexpected sudden deflection, or have retract curves that do not have a constant slope.

For homogeneous 2D substrates and acellular 3D hydrogels, the protocol will generate values for *E*, which will often be normally distributed. For example, in Fig. 5b, we calculated a median *E* of ~ 500 Pa for acellular S-HA-PEGDA hydrogels formed with a weight ratio of S-HA-PEGDA of 1:3[21]. Similarly, the *E* of PA hydrogels is expected to vary in line with changing the concentrations of the monomer and cross-linker base components. In Fig. 5c, we probed the surface of PA hydrogels formed with either 75 µL/30 µL or 200 µL/240 µL acrylamide/bis-acrylamide ratios and measured median *E* of 0.167 (0.161 - 0.170 95% CI) and 49.6 (48.1 - 50.5 95% CI) kPa, respectively. We then used these surfaces to determine that in hMSC undergoing chondrogenesis, hypoxia's effects are modulated, at least in part, by mechanosensitive pathways[16].

For samples containing encapsulated cells or organoids, and particularly in samples that have undergone cell-mediated remodelling of their surroundings, *E* may not be normally distributed. Here, differential matrix remodelling activity can be inferred from the variance and/or distribution of data plots. For example, in Fig. 5b, histograms show multiple/broadened peaks in cell-laden compared to acellular S-HA-PEGDA hydrogels. For cell-laden hydrogels, unsupervised peak fitting of the bi-modal distribution of *E* detected one value of *E* that was no different from that of acellular controls, and another that was stiffer. Moreover, the presence of cells significantly affected the distribution of *E.* Indeed, a Mantel-Haenszel linear-by-linear association Chi-square test for trend yielded a $\chi^2 = 79.170$ ($p < 0.001$), and a non-parametric Goodman and Kruskal's gamma of $\gamma = 0.448$ ($p < 0.001$). Analysis of standardized residuals further identified areas of the histograms that most attributed to differences within the following bins: 501-1,000; 4,001-5,000; 5,501-6,500. Using mechanistic approaches to inhibit protein secretion by encapsulated cells, we were able to show that these changes in the distribution of *E* could be attributed to cell-mediated matrix remodelling[21], which we went onto conclude could impact the differentiation of encapsulated hMSC.

In PEG hydrogels containing encapsulated human intestinal organoids (HIO), we have similarly used this protocol to infer peri-organoid matrix remodelling. HIO contain both epithelial and mesenchymal cells. We co-cultured HIO encapsulated within PEG hydrogels with type I innate lymphoid cells (ILC1), a source of TGFβ1 and MMP9, and were able to detect significantly greater variance in measurements of E^{23} in the ILC1 co-culture group compared to controls. Indeed, violin plots (Fig. 5e) and maps (Fig. 5d) of *E* collected across the hydrogel surface, both showed significantly more variability, which we were able to confirm using a Kolmogorov-Smirnov test. Here, maps of *E* were collected directly over encapsulated organoids (epithelial, Ep and fibroblast, Fb highlighted in images) and plotted as heat maps. We then linked this increased variation in measurements of *E* to both an increase in fibronectin expression and MMP9 activity in the co-culture group. These findings revealed an unexpected role for ILC1 in modulating matrix remodelling in the intestine.

Figure legends

Figure 1: The influence of matrix stiffness and cell-pericellular matrix interactions on cellular behaviours.
On stiff substrates (**a**) cells spread and exert traction forces on the surrounding material, but on soft substrates (**b**) cells adopt round morphologies and are more motile. In 3D hydrogels, encapsulated single cells (**c**) and cell clusters or organoids (**d**) can actively remodel their peri-cellular environment by secreting enzymes (*e.g.*, MMPs) to degrade the matrix, and by producing and depositing native extracellular matrix proteins.

Figure 2: Concept for measuring relative differences between 3D cell structures embedded within 3D hydrogels.
Schematic of cell clusters or organoids encapsulated within a hydrogel. As the hydrogel is indented, the AFM probe detects the stiffness of a combination of both the hydrogel and the underlying organoid. As encapsulated cells/organoids remodel their surrounding environment through matrix degradation (left) and ECM production (right), AFM force spectroscopy measurements can detect these effects as changes in *E*. This allows for relative comparisons of matrix changes between identical hydrogel conditions with defined mechanical properties.

Figure 3: AFM setup and procedure for carrying out *F-D* measurements.
(**a**) Image of a cantilever holder, showing the cantilever tip positioned over the polished glass through which the laser light passes. (**b**) Schematic showing how to mount a bead on a cantilever: Beads are placed on a glass slide alongside a drop of UV-curable glue. (Steps 12,13) The cantilever tip is lowered onto the glue to apply a small amount of glue to the tip (Step 18), it is then retracted (Step 19), and is moved over and lowered onto a single bead (Step 21). Once a single bead is attached to the cantilever, the cantilever is placed under a UV lamp to cure the glue (Step 24). Images show what the user will see on the AFM when mounting the bead on the cantilever. Scale bar = 100 µm. (**c**) Schematic showing how various samples can be mounted for measurements. A free-floating 3D hydrogel can be held in place using coverslips glued to the base of a dish (top), a 2D hydrogel can be adhered to a glass slide and submersed in solution (middle), or a 2D surface can be attached to a glass coverslip (bottom). (**d**) Schematic showing how *F-D* curves can be collected automatically to create a 10x10 map.

Figure 4: *F-D* curve interpretation and modelling.
Schematic of a typical *F-D* curve showing the cantilever approach (blue) and retraction (red) from a sample. P_{max} is the maximum load, and *E* is calculated using either the slope (dy/dx, N/m) of the *Retract* curve (red) curve using Oliver-Pharr model or the slope of the *Extend* curve (blue) using Hertz model. The indentation depth (H_{max}) is calculated as the distance from the contact point on the *Extend* curve to the maximum displacement (m) at P_{max}.

Figure 5: Anticipated results.
(**a**) Representative accepted *F–D* curves (left), and example curves that were not analyzed (right) collected on acellular 3D PEG hydrogels[23]. *F-D* curves were collected using tipless triangular silicon nitride cantilevers (*K*=0.12N/m) functionalized with a 10µm silica bead, at a relative setpoint of 3 nN and approach speed of 4µm/s. Curves were rejected if there was not a smooth retract/extend curve, for excessive adhesion between the tip and sample, or for too

much noise. (**b**) Young's modulus (*E*, Pa) of acellular and cell-laden 3D S-HA-PEGDA hydrogels after 3 days in culture[21]. *F-D* curves were collected using tipless triangular silicon nitride cantilevers (*K*=0.12N/m) functionalized with a 55 μm glass bead at a loading rate of 30μm/s (mean indentation depth, 1.15μm). *F-D* curves were analyzed using the Oliver-Pharr model. Box-whisker plots of *E* show the median (central line), 1st and 3rd quartiles (bounds of box), and high and low values (whiskers). Mann-Whitney test (two-tailed) (***$p < 0.001$). Histograms show distributions of *E* with insets showing distributions and fitted normal distributions, with centre of peak ± standard deviation. (**c**) Plots show Young's modulus (*E*, kPa) of soft, 75/30 and stiff, 200/240 (acrylamide/bis-acrylamide) polyacrylamide hydrogels[16]. *F-D* curves were collected using tipless triangular silicon nitride cantilevers (*K*=0.12N/m) functionalized with 10μm diameter silica bead at a loading rate of 4μm/s (indentation depth of 1-1.5 μm). Each dot represents one *F-D* measurement, with 1151 measurements of 2 independent soft gels and 1169 measurements on 2 independent stiff gels. *E* was calculated using the Oliver-Pharr model. The horizontal line shows the median and error bars show the interquartile range. (**d**) Representative 150μmx150μm stiffness maps collected above HIO encapsulated in intermediately-degradable (45% MMP-sensitive, ~1 kPa) PEG hydrogels[23]. HIO were encapsulated without or with type-1 innate lymphoid cells (ILC), a source of TGFβ1 and MMP9. Black outlines delineate approximate locations of the epithelial layer (Ep) and surrounding fibroblast region (Fb), both visible in the phase contrast images (insets, scale bar=100μm). White/x squares denote omitted measurements that failed to meet QC standards. *F-D* measurements were collected at a relative setpoint of 2.5nN and a loading rate of 4μm/s using a tipless triangular silicon nitride cantilever (*K*=0.12N/m) functionalized with a 50μm diameter glass bead. (**e**) Violin plots summarize measurements of *E* (Hertz model) on HIO-laden gels measured directly above HIO with or without ILC. Measurements were carried out as described in (d). Red lines show the median and blue lines indicate 1st and 3rd quartiles. Data sets were compared using a non-parametric Kolmogorov-Smirnov test (Approximate $p = 0.0011$, 50-70 measurements per force map, N=3 independent maps).

ACKNOWLEDGMENTS
MDAN acknowledges funding from the London Interdisciplinary Doctoral Programme, which is funded by the BBSRC. SAF acknowledges a Springboard Fellowship from the Imperial College London Institutional Strategic Support Fund, which was established with funding from the Wellcome Trust. GMJ acknowledges a PhD studentship from the Wellcome Trust (203757/Z/16/A). LB acknowledges funding from a University College London Impact Award and industrial sponsorships. EG acknowledges a Philip Leverhulme Prize from the Leverhulme Trust. This work was part funded by generous support from the Rosetrees Trust. The authors are especially grateful for technical support from Dr. Richard Thorogate at London Centre for Nanotechnology and to Dr Suzette T. Lust for helpful conversations regarding the MatLab code.

AUTHORS CONTRIBUTIONS
MDAN, SAF and GMJ developed experimental protocols, designed and conducted experiments, and analyzed the data. MDAN, SAF, GMJ, LB and EG conceived the ideas and contributed to experimental interpretation. All authors wrote and revised the manuscript.

COMPETING INTERESTS
The authors declare no competing interests.

DATA AVAILABILITY
All data presented in Fig. 5 are available within the supporting primary research articles Foyt et al.16 Ferreira et al. 21 Jowett et al. 23, or are available from the corresponding author upon reasonable request.

CODE AVAILABILITY
The Matlab code described in this manuscript is freely available at https://github.com/eileengentleman/AFM-code. **[AU: Please make sure that the code is made available at this stage.]**

RELATED LINKS

Key references using this protocol:

1. Ferreira, S. A. *et al. Nat. Commun.* 9, 4049 (2018). https://doi.org/10.1038/s41467-018-06183-4
2. Foyt, D. A. *et al. Acta Biomater.* (2019). https://doi.org/10.1016/j.actbio.2019.03.002
3. Jowett, G. M. *et al. Nat. Mater.* (2020). https://doi.org/10.1038/s41563-020-0783-8

SUPPLEMENTARY INFORMATION

- **Supplementary Note 1: Background on Oliver and Pharr model and further instructions for use of code.**
-

REFERENCES

1. Evans, N. D. & Gentleman, E. The role of material structure and mechanical properties in cell-matrix interactions. *J. Mater. Chem. B* **2,** 2345-2356 (2014).
2. Engler, A. J., Sen, S., Sweeney, H. L. & Discher, D. E. Matrix elasticity directs stem cell lineage specification. *Cell* **126,** 677-689 (2006).
3. Evans, N. D. *et al.* Substrate stiffness affects early differentiation events in embryonic stem cells. *Eur. Cell. Mater.* **18,** 1-14 (2009).
4. Krishnan, R. *et al.* Substrate stiffening promotes endothelial monolayer disruption through enhanced physical forces. *Am. J. Physiol. Cell Physiol.* **300,** C146-154 (2011).
5. Mammoto, A., Mammoto, T. & Ingber, D. E. Mechanosensitive mechanisms in transcriptional regulation. *J. Cell Sci.* **125,** 3061-3073 (2012).
6. Engler, A. J. *et al.* Myotubes differentiate optimally on substrates with tissue-like stiffness: pathological implications for soft or stiff microenvironments. *J. Cell. Biol.* **166,** 877-887 (2004).
7. Wells, R. G. The role of matrix stiffness in regulating cell behavior. *Hepatology* **47,** 1394-1400 (2008).
8. Levental, K. R. *et al.* Matrix crosslinking forces tumor progression by enhancing integrin signaling. *Cell* **139,** 891-906 (2009).
9. Martin, L. J. & Boyd, N. F. Mammographic density. Potential mechanisms of breast cancer risk associated with mammographic density: hypotheses based on epidemiological evidence. *Breast Cancer Res.* **10,** 201-215 (2008).
10. Wei, S. C. *et al.* Matrix stiffness drives epithelial-mesenchymal transition and tumour metastasis through a TWIST1-G3BP2 mechanotransduction pathway. *Nat. Cell Biol.* **17,** 678 (2015).
11. Baumgart, F. Stiffness - an unknown world of mechanical science? *Injury* **31,** 14-84 (2000).
12. Thompson, D. W., *On growth and form*, 1942 edition ed. (Cambridge University Press, 1917).
13. Emerman, J. T. & Pitelka, D. R. Maintenance and induction of morphological differentiation in dissociated mammary epithelium on floating collagen membranes. *In Vitro* **13,** 316-328 (1977).
14. Pelham, R. J. & Wang, Y. Cell locomotion and focal adhesions are regulated by substrate flexibility. *Proc. Natl. Acad. Sci. USA* **94,** 13661-13665 (1997).
15. Discher, D. E., Janmey, P. & Wang, Y. L. Tissue cells feel and respond to the stiffness of their substrate. *Science* **310,** 1139-1143 (2005).
16. Foyt, D. A. *et al.* Hypoxia impacts human MSC response to substrate stiffness during chondrogenic differentiation. *Acta Biomater.* **15,** 73-83 (2019).
17. Chin, M. H. W. *et al.* A hydrogel-integrated culture device to interrogate T cell activation with physicochemical cues. *ACS Appl. Mater. Interfaces* **12,** 47355–47367 (2020).
18. Huebsch, N. *et al.* Harnessing traction-mediated manipulation of the cell/matrix interface to control stem-cell fate. *Nat. Mater.* **9,** 518-526 (2010).
19. Khetan, S. *et al.* Degradation-mediated cellular traction directs stem cell fate in covalently crosslinked three-dimensional hydrogels. *Nat. Mater.* **12,** 458-465 (2013).
20. Blache, U., Stevens, M. M. & Gentleman, E. Harnessing the secreted matrix to engineer tissues. *Nat. Biomed. Eng.* **4,** 357-363 (2020).

21. Ferreira, S. A. *et al.* Bi-directional cell-pericellular matrix interactions direct stem cell fate. *Nat. Commun.* **9,** 4049 (2018).
22. Loebel, C., Mauck, R. L. & Burdick, J. A. Local nascent protein deposition and remodelling guide mesenchymal stromal cell mechanosensing and fate in three-dimensional hydrogels. *Nat. Mater.* **18,** 883-891 (2019).
23. Jowett, G. M. *et al.* ILC1 drive intestinal epithelial and matrix remodelling. *Nat. Mater.* (2020).
24. Barriga, E. H., Franze, K., Charras, G. & Mayor, R. Tissue stiffening coordinates morphogenesis by triggering collective cell migration in vivo. *Nature* **554,** 523-527 (2018).
25. Gilbert, P. M. *et al.* Substrate elasticity regulates skeletal muscle stem cell self-renewal in culture. *Science* **329,** 1078-1081 (2010).
26. McKee, C. T., Last, J. A., Russell, P. & Murphy, C. J. Indentation versus tensile measurements of Young's modulus for soft biological tissues. *Tissue Eng. Part B Rev.* **17,** 155-164 (2011).
27. Denisin, A. K. & Pruitt, B. L. Tuning the range of polyacrylamide gel stiffness for mechanobiology applications. *ACS Appl. Mater. Interfaces* **8,** 21893-21902 (2016).
28. Prager-Khoutorsky, M. *et al.* Fibroblast polarization is a matrix-rigidity-dependent process controlled by focal adhesion mechanosensing. *Nat. Cell Biol.* **13,** 1457-1465 (2011).
29. Trappmann, B. *et al.* Extracellular-matrix tethering regulates stem-cell fate. *Nat. Mater.* **11,** 642-649 (2012).
30. Wen, J. H. *et al.* Interplay of matrix stiffness and protein tethering in stem cell differentiation. *Nat. Mater.* **13,** 979-987 (2014).
31. Krieg, M. *et al.* Atomic force microscopy-based mechanobiology. *Nat. Rev. Phys.* **1,** 41-57 (2019).
32. Megone, W., Roohpour, N. & Gautrot, J. E. Impact of surface adhesion and sample heterogeneity on the multiscale mechanical characterisation of soft biomaterials. *Sci. Rep.* **8,** 6780 (2018).
33. Schultz, K. M. & Furst, E. M. Microrheology of biomaterial hydrogelators. *Soft Matter* **8,** 6198-6205 (2012).
34. Ziemann, F., Radler, J. & Sackmann, E. Local measurements of viscoelastic moduli of entangled actin networks using an oscillating magnetic bead micro-rheometer. *Biophys. J.* **66,** 2210-2216 (1994).
35. Campas, O. *et al.* Quantifying cell-generated mechanical forces within living embryonic tissues. *Nat. methods* **11,** 183-189 (2014).
36. Wang, S. & Larin, K. V. Optical coherence elastography for tissue characterization: a review. *J Biophotonics* **8,** 279-302 (2015).
37. Scarcelli, Giuliano & Yun, Seok Hyun Confocal Brillouin microscopy for three-dimensional mechanical imaging. *Nat. Photonics* **2,** 39-43 (2007).
38. Shi, Y. *et al.* Feasibility of using 3D MR elastography to determine pancreatic stiffness in healthy volunteers. *J. Magn. Reson. Imaging* **41,** 369-375 (2015).
39. Anvari, A., Dhyani, M., Stephen, A. E. & Samir, A. E. Reliability of shear-wave elastography estimates of the young modulus of tissue in follicular thyroid neoplasms. *Am. J. Roentgenol.* **206,** 609-616 (2016).
40. Schultz, K.M., Kyburz, K. A. & Anseth, K. S. Measuring dynamic cell-material interactions and remodeling during 3D human mesenchymal stem cell migration in hydrogels. *Proc. Natl. Acad. Sci. USA* **112,** E3757 (2015).
41. Yofe, A. D. Physics at surfaces. *Contemp. Phys.* **29,** 411-414 (1988).
42. Flory, P. J., *Principles of polymer chemistry*. (Cornell University Press, 1953).

43. Offeddu, G. S., Axpe, E., Harley, B. A. C. & Oyen, M. L. Relationship between permeability and diffusivity in polyethylene glycol hydrogels. *AIP Adv.* **8,** 105006 (2018).
44. Oyen, M. L. Nanoindentation of hydrated materials and tissues. *Curr. Opin. Solid State Mater. Sci.* **19,** 317-323 (2015).
45. Schillers, H. *et al.* Standardized nanomechanical atomic force microscopy procedure (SNAP) for measuring soft and biological samples. *Sci. Rep.* **7,** 5117 (2017).
46. Sader, J. E., Chon, J. W. M. & Mulvaney, P. Calibration of rectangular atomic force microscope cantilevers. *Rev. Sci. Instrum.* **70,** 3967-3969 (1999).
47. Cleveland, J. P., Manne, S., Bocek, D. & Hansma, P. K. A nondestructive method for determining the spring constant of cantilevers for scanning force microscopy. *Rev. Sci. Instrum.* **64,** 403-405 (1993).
48. Torii, A., Sasaki, M., Hane, K. & Okuma, S. A method for determining the spring constant of cantilevers for atomic force microscopy. *Meas. Sci. Technol.* **7,** 179-184 (1996).
49. Gibson, C. T., Watson, G. S. & Myhra, S. Determination of the spring constants of probes for force microscopy/spectroscopy. *Nanotechnology* **7,** 259-262 (1996).
50. Gates, R.S. & Reitsma, M. G. Precise atomic force microscope cantilever spring constant calibration using a reference cantilever array. *Rev. Sci. Instrum.* **78,** 086101 (2007).
51. Hutter, J. L. & Bechhoefer, J. Calibration of atomic-force microscope tips. *Rev. Sci. Instrum.* **64,** 1868-1873 (1993).
52. Palacio, M. L. B. & Bhushan, B. Normal and lateral force calibration techniques for AFM cantilevers. *Crit. Rev. Solid State Mater. Sci.* **35,** 73-104 (2010).
53. Lin, D. C. & Horkay, F. Nanomechanics of polymer gels and biological tissues: A critical review of analytical approaches in the Hertzian regime and beyond. *Soft Matter* **4,** 669-682 (2008).
54. Oyen, M. L. & Cook, R. F. A practical guide for analysis of nanoindentation data. *J. Mech. Behav. Biomed. Mater.* **2,** 396-407 (2009).
55. Oliver, W. C. & Pharr, G. M. An improved technique for determining hardness and elastic modulus using load and displacement sensing indentation experiments. *J. Mater. Res.* **7,** 1564-1583 (1992).
56. Kohn, J. C. & Ebenstein, D. M. Eliminating adhesion errors in nanoindentation of compliant polymers and hydrogels. *J. Mech. Behav. Biomed. Mater.* **20,** 316-326 (2013).
57. Li, M., Liu, L., Xi, N. & Wang, Y. Nanoscale monitoring of drug actions on cell membrane using atomic force microscopy. *Acta Pharmacol. Sin.* **36,** 769-782 (2015).
58. Gautier, H. O. B. *et al.*,Chapter 12 - Atomic force microscopy-based force measurements on animal cells and tissues. In *Methods in Cell Biology.* (Academic Press, 2015), Vol. 125, pp. 211-235.
59. Staunton, J. R., Doss, B. L., Lindsay, S. & Ros, R. Correlating confocal microscopy and atomic force indentation reveals metastatic cancer cells stiffen during invasion into collagen I matrices. *Sci. Rep.* **6,** 19686 (2016).
60. Rheinlaender, J. *et al.* Cortical cell stiffness is independent of substrate mechanics. *Nat. Mater.* **19,** 1019–1025 (2020).
61. Loebel, C. *et al.* Metabolic labeling to probe the spatiotemporal accumulation of matrix at the chondrocyte-hydrogel interface. *Adv. Funct. Mater.*1909802 (2020).
62. Dimitriadis, E. K. *et al.* Determination of elastic moduli of thin layers of soft material using the atomic force microscope. *Biophys. J.* **82,** 2798-2810 (2002).
63. Selby, A., Maldonado-Codina, C. & Derby, B. Influence of specimen thickness on the nanoindentation of hydrogels: measuring the mechanical properties of soft contact lenses. *J. Mech. Behav. Biomed. Mater.* **35,** 144-156 (2014).

64. Jung, Y. G. *et al.* Evaluation of elastic modulus and hardness of thin films by nanoindentation. *J. Mater. Res.* **19,** 3076-3080 (2004).
65. Sirghi, L., Ponti, J., Broggi, F. & Rossi, F. Probing elasticity and adhesion of live cells by atomic force microscopy indentation. *Eur. Biophys. J.* **37,** 935-945 (2008).
66. Buxboim, A., Rajagopal, K., Brown, A. E. & Discher, D. E. How deeply cells feel: methods for thin gels. *J. Phys. Condens. Matter.* **22,** 194116 (2010).
67. Tusan, C. G. *et al.* Collective cell behavior in mechanosensing of substrate thickness. *Biophys. J.* **114,** 2743-2755 (2018).
68. Carrillo, F. *et al.* Nanoindentation of polydimethylsiloxane elastomers: Effect of crosslinking, work of adhesion, and fluid environment on elastic modulus. *J. Mater. Res.* **20,** 2820-2830 (2005).
69. Garcia, P. D., Guerrero, C. R. & Garcia, R. Nanorheology of living cells measured by AFM-based force-distance curves. *Nanoscale* **12,** 9133-9143 (2020).
70. Efremov, Y. M., Okajima, T. & Raman, A. Measuring viscoelasticity of soft biological samples using atomic force microscopy. *Soft Matter* **16,** 64-81 (2020).
71. Ledeczi, A. & Fitzpatricl, M., Introduction to programming with MATLAB, Available at https://www.coursera.org/learn/matlab, (2020).
72. JPKInstruments, Determining the elastic modulus of biological samples using atomic force microscopy, Available at https://www.jpk.com/app-technotes-img/AFM/pdf/jpk-app-elastic-modulus.14-1.pdf, (2020).
73. Tse, J. R. & Engler, A. J. Preparation of hydrogel substrates with tunable mechanical properties. *Curr. Protoc. Stem Cell Biol.* **47,** 10.16.11-10.16.16 (2010).
74. Shu, X. Z. *et al.* Disulfide cross-linked hyaluronan hydrogels. *Biomacromolecules* **3,** 1304-1311 (2002).
75. Ferreira, S. A. *et al.* Neighboring cells override 3D hydrogel matrix cues to drive human MSC quiescence. *Biomaterials* **176,** 13-23 (2018).
76. Kloxin, A. M., Kasko, A. M., Salinas, C. N. & Anseth, K. S. Photodegradable hydrogels for dynamic tuning of physical and chemical properties. *Science* **324,** 59 (2009).
77. Lutolf, M. P. *et al.* Synthetic matrix metalloproteinase-sensitive hydrogels for the conduction of tissue regeneration: Engineering cell-invasion characteristics. *Proc. Natl. Acad. Sci. USA* **100,** 5413 (2003).
78. McCracken, K. W., Howell, J. C., Wells, J. M. & Spence, J. R. Generating human intestinal tissue from pluripotent stem cells in vitro. *Nat. Protoc.* **6,** 1920-1928 (2014).
79. Burnham, N. A. *et al.* Comparison of calibration methods for atomic-force microscopy cantilevers. *Nanotechnology* **14,** 1-6 (2003).
80. Kain, L. *et al.* Calibration of colloidal probes with atomic force microscopy for micromechanical assessment. *J. Mech. Behav. Biomed. Mater.* **85,** 225-236 (2018).
81. Chighizola, M., Puricelli, L., Bellon, L. & Podestà, A. Large colloidal probes for atomic force microscopy: fabrication and calibration issues. *arXiv:2007.15112* (2020).
82. Butt, H. J. & Jaschke, M. Calculation of thermal noise in atomic force microscopy. *Nanotechnology* **6,** 1-7 (1995).

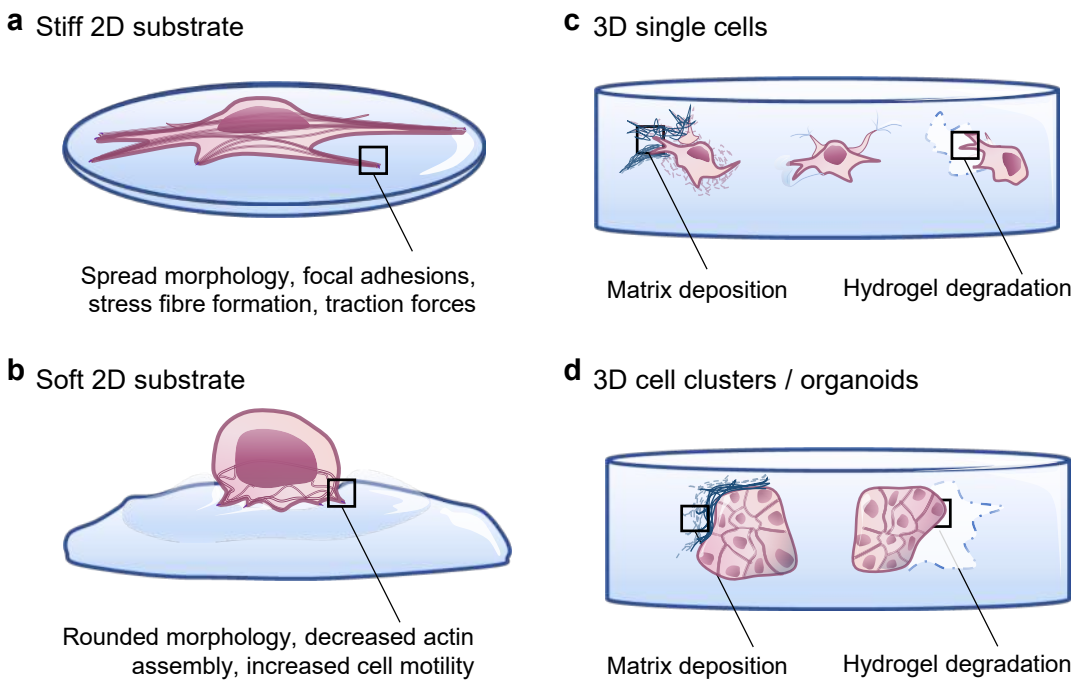

Figure 1: The influence of matrix stiffness and cell-pericellular matrix interactions on cellular behaviours.

On stiff substrates (**a**) cells spread and exert traction forces on the surrounding material, but on soft substrates (**b**) cells adopt round morphologies and are more motile. In 3D hydrogels, encapsulated single cells (**c**) and cell clusters or organoids (**d**) can actively remodel their peri-cellular environment by secreting enzymes (*e.g.*, MMPs) to degrade the matrix, and by producing and depositing native extracellular matrix proteins.

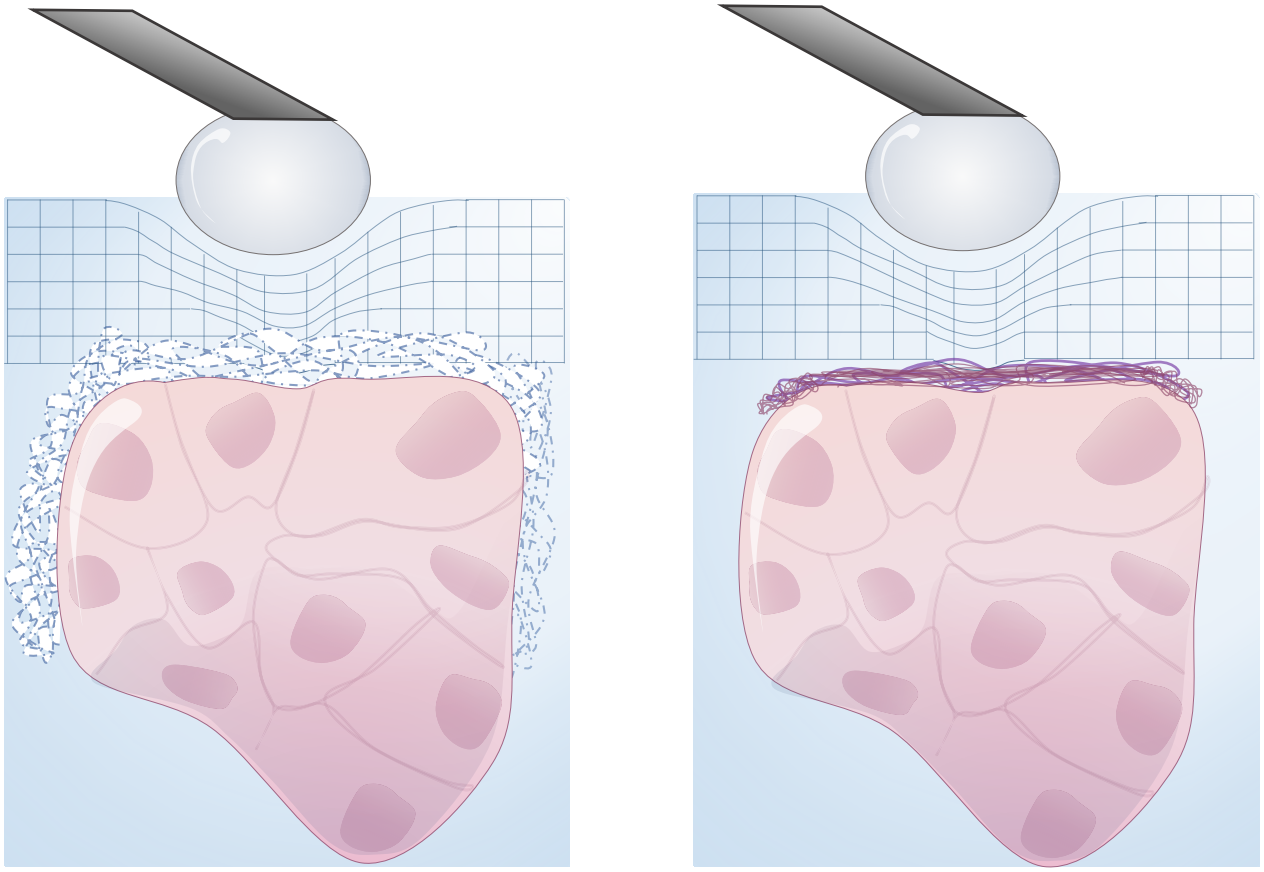

Figure 2: Concept for measuring relative differences between 3D cell structures embedded within 3D hydrogels.

Schematic of cell clusters or organoids encapsulated within a hydrogel. As the hydrogel is indented, the AFM probe detects the stiffness of a combination of both the hydrogel and the underlying organoid. As encapsulated cells/organoids remodel their surrounding environment through matrix degradation (left) and ECM production (right), AFM force spectroscopy measurements can detect these effects as changes in *E*. This allows for relative comparisons of matrix changes between identical hydrogel conditions with defined mechanical properties.

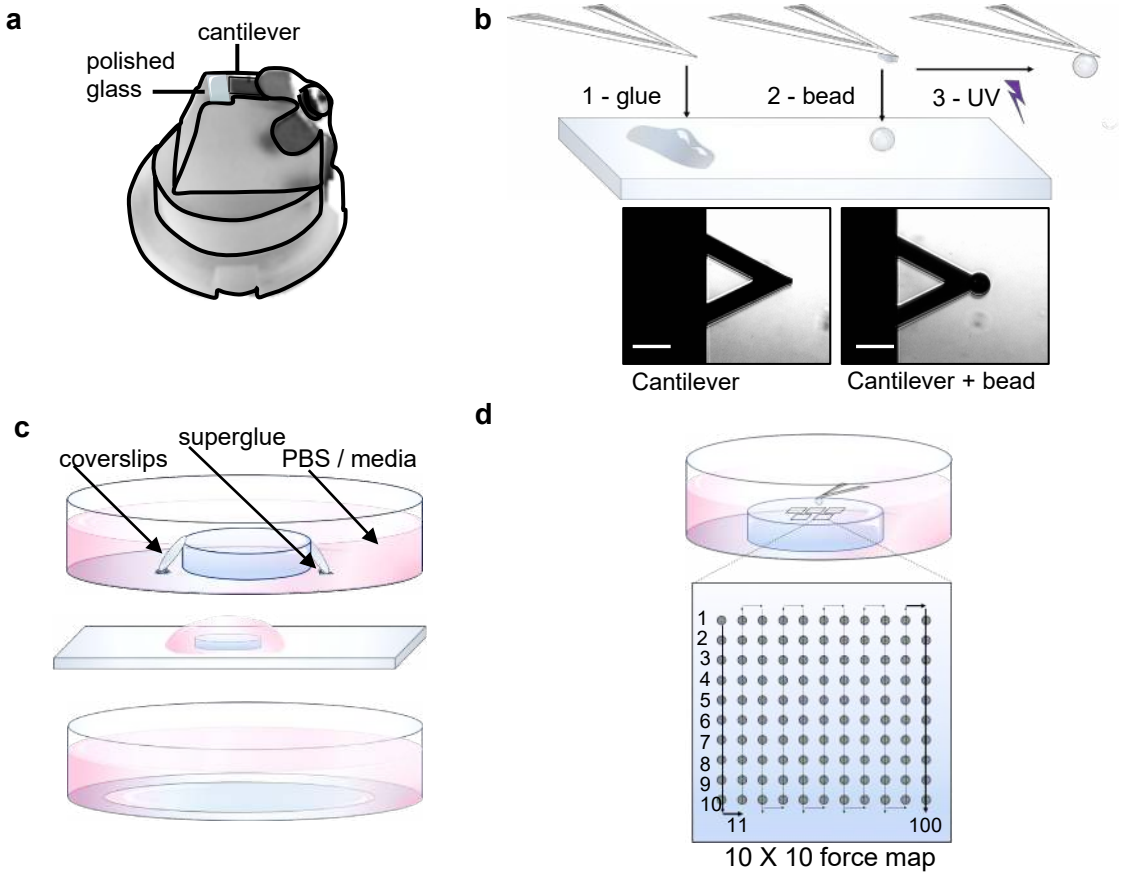

Figure 3: AFM setup and procedure for carrying out *F-D* measurements.
(**a**) Image of a cantilever holder, showing the cantilever tip positioned over the polished glass through which the laser light passes. (**b**) Schematic showing how to mount a bead on a cantilever: Beads are placed on a glass slide alongside a drop of UV-curable glue. (Steps 12,13) The cantilever tip is lowered onto the glue to apply a small amount of glue to the tip (Step 18), it is then retracted (Step 19), and is moved over and lowered onto a single bead (Step 21). Once a single bead is attached to the cantilever, the cantilever is placed under a UV lamp to cure the glue (Step 24). Images show what the user will see on the AFM when mounting the bead on the cantilever. Scale bar = 100 µm. (**c**) Schematic showing how various samples can be mounted for measurements. A free-floating 3D hydrogel can be held in place using coverslips glued to the base of a dish (top), a 2D hydrogel can be adhered to a glass slide and submersed in solution (middle), or a 2D surface can be attached to a glass coverslip (bottom). (**d**) Schematic showing how *F-D* curves can be collected automatically to create a 10x10 map.

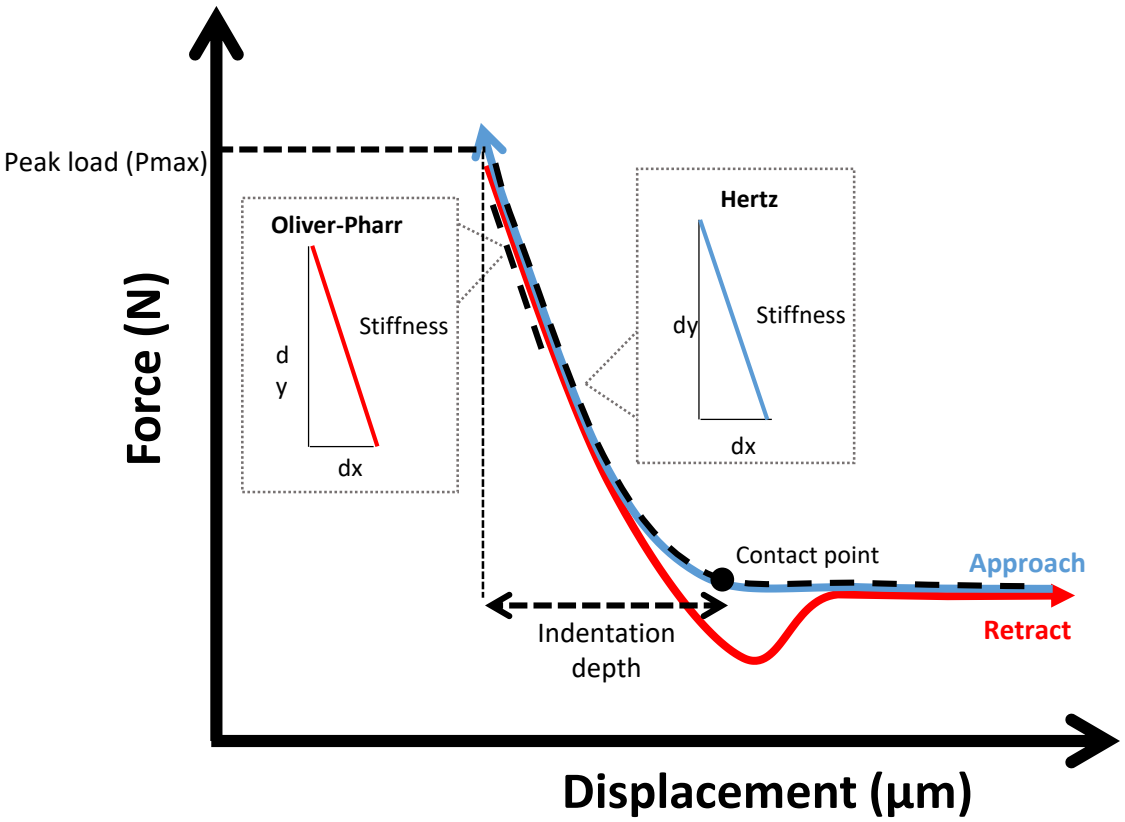

Figure 4: *F-D* curve interpretation and modelling.
Schematic of a typical *F-D* curve showing the cantilever approach (blue) and retraction (red) from a sample. P_{max} is the maximum load, and *E* is calculated using either the slope (dy/dx, N/m) of the *Retract* curve (red) curve using Oliver-Pharr model or the slope of the *Extend* curve (blue) using Hertz model. The indentation depth (H_{max}) is calculated as the distance from the contact point on the *Extend* curve to the maximum displacement (m) at P_{max}.

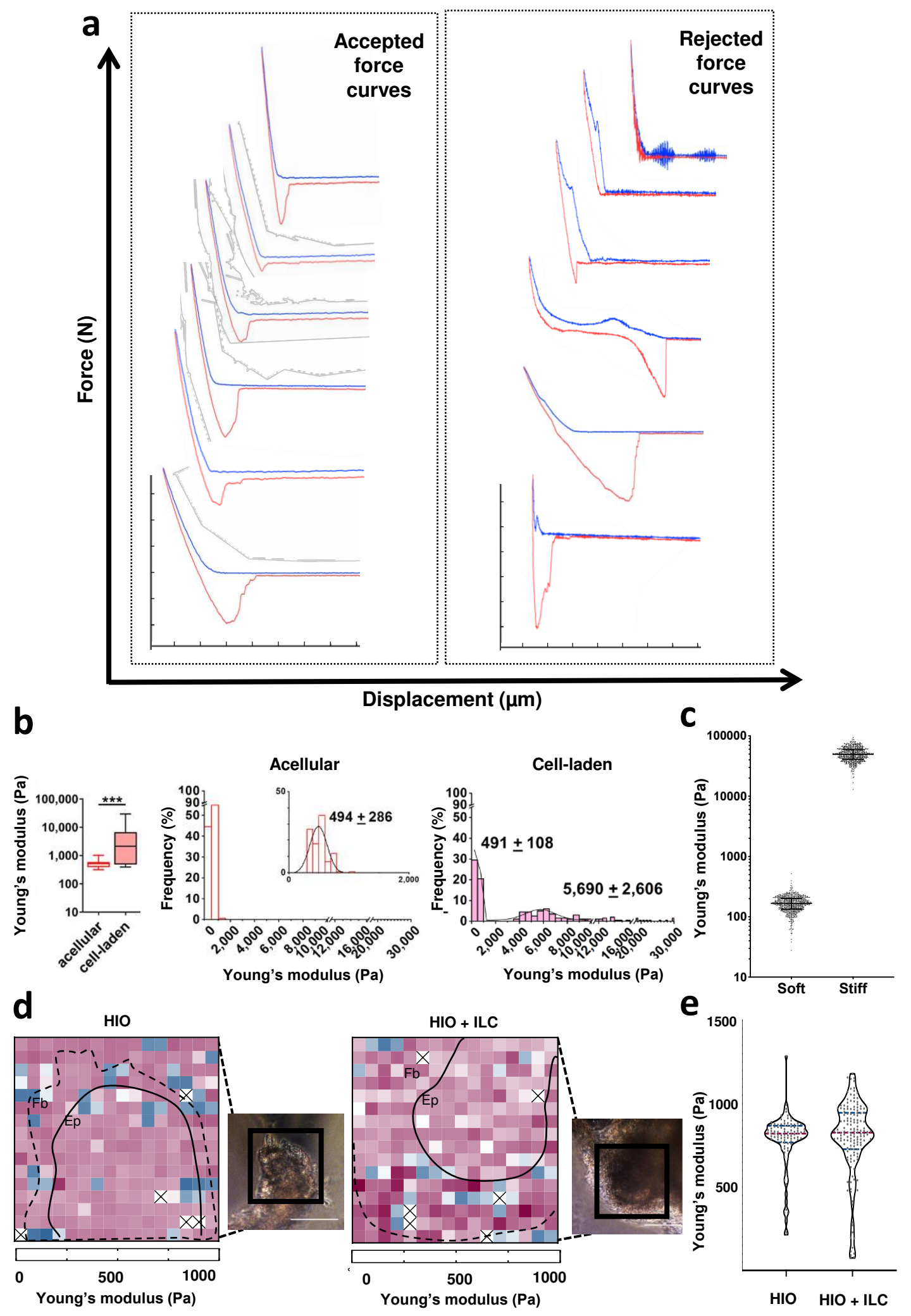
a
Accepted force curves
Rejected force curves
Force (N)
Displacement (μm)
b
Young's modulus (Pa)
***
acellular
cell-laden
Acellular
Cell-laden
Frequency (%)
494 ± 286
491 ± 108
5,690 ± 2,606
Young's modulus (Pa)
c
Young's modulus (Pa)
Soft
Stiff
d
HIO
HIO + ILC
Fb
Ep
0
500
1000
Young's modulus (Pa)
e
Young's modulus (Pa)
1500
1000
500
HIO
HIO + ILC

Figure 5: Anticipated results.

(**a**) Representative accepted *F–D* curves (left), and example curves that were not analyzed (right) collected on acellular 3D PEG hydrogels[23]. *F-D* curves were collected using tipless triangular silicon nitride cantilevers (*K*=0.12N/m) functionalized with a 10µm silica bead, at a relative setpoint of 3 nN and approach speed of 4µm/s. Curves were rejected if there was not a smooth retract/extend curve, for excessive adhesion between the tip and sample, or for too much noise. (**b**) Young's modulus (*E*, Pa) of acellular and cell-laden 3D S-HA-PEGDA hydrogels after 3 days in culture[21]. *F-D* curves were collected using tipless triangular silicon nitride cantilevers (*K*=0.12N/m) functionalized with a 55 µm glass bead at a loading rate of 30µm/s (mean indentation depth, 1.15µm). *F-D* curves were analyzed using the Oliver-Pharr model. Box-whisker plots of *E* show the median (central line), 1st and 3rd quartiles (bounds of box), and high and low values (whiskers). Mann-Whitney test (two-tailed) (***$p < 0.001$). Histograms show distributions of *E* with insets showing distributions and fitted normal distributions, with centre of peak ± standard deviation. (**c**) Plots show Young's modulus (*E*, kPa) of soft, 75/30 and stiff, 200/240 (acrylamide/bis-acrylamide) polyacrylamide hydrogels[16]. *F-D* curves were collected using tipless triangular silicon nitride cantilevers (*K*=0.12N/m) functionalized with 10µm diameter silica bead at a loading rate of 4µm/s (indentation depth of 1-1.5 µm). Each dot represents one *F-D* measurement, with 1151 measurements of 2 independent soft gels and 1169 measurements on 2 independent stiff gels. *E* was calculated using the Oliver-Pharr model. The horizontal line shows the median and error bars show the interquartile range. (**d**) Representative 150µmx150µm stiffness maps collected above HIO encapsulated in intermediately-degradable (45% MMP-sensitive, ~1 kPa) PEG hydrogels[23]. HIO were encapsulated without or with type-1 innate lymphoid cells (ILC), a source of TGFβ1 and MMP9. Black outlines delineate approximate locations of the epithelial layer (Ep) and surrounding fibroblast region (Fb), both visible in the phase contrast images (insets, scale bar=100µm). White/x squares denote omitted measurements that failed to meet QC standards. *F-D* measurements were collected at a relative setpoint of 2.5nN and a loading rate of 4µm/s using a tipless triangular silicon nitride cantilever (*K*=0.12N/m) functionalized with a 50µm diameter glass bead. (**e**) Violin plots summarize measurements of *E* (Hertz model) on HIO-laden gels measured directly above HIO with or without ILC. Measurements were carried out as described in (d). Red lines show the median and blue lines indicate 1st and 3rd quartiles. Data sets were compared using a non-parametric Kolmogorov-Smirnov test (Approximate $p = 0.0011$, 50-70 measurements per force map, N=3 independent maps).